1966

A theoretical analysis of the effect of the modulus of elasticity and other parameters upon the flutter of a helicopter rotor blade in hovering flight.

Swah, Samuel Ryan.

Princeton University

A THEORETICAL ANALYSIS OF THE EFFECT OF THE MODULUS OF ELASTICITY AND OTHER PARAMETERS UPON THE FLUTTER OF A HELICOPTER ROTOR BLADE IN HOVERING FLIGHT

****

Samuel Ryan Swah

Princeton University.
School of Engineering and Applied Science
Aerospace and Mechanical Sciences Department

A THEORETICAL ANALYSIS OF THE EFFECT OF THE MODULUS OF ELASTICITY AND OTHER PARAMETERS UPON THE FLUTTER OF A HELICOPTER ROTOR BLADE IN HOVERING FLIGHT

by

Samuel Ryan Swah

Department of Aerospace and Mechanical Sciences
Princeton University

September 1971

Submitted in partial fulfillment of the requirements
for the degree of Master of Science in Engineering

ACKNOWLEDGEMENT

Grateful acknowledgement is made of the knowledge and assistance afforded me by Professor H. C. Curtiss, Jr. and Mr. William F. Putman of the Dynamic Model Track of Princeton University. Also, the advice and help of Professor V. V. Utgoff of the United States Naval Academy was of immense help.

Thanks also goes to Miss Mary Ann Mamo for her patience in the typing of this report.

This thesis carries No. 1003 - T in the records of the Department of Aerospace and Mechanical Sciences.

TABLE OF CONTENTS

NOMENCLATURE

a	- blade section lift curve slope. per radian
A.C.	- aerodynamic center
$C'(k)$	- lift deficiency function, including blade wake effects
C.G.	- center of gravity
c	- blade section chord
E	- blade bending modulus of elasticity
E.E.	- elastic axis
g_k	- displacement of blade k bending mode
I	- blade section second moment of area, flatwise bending, or $\frac{I_f}{I_b}$
I_b	- blade moment of inertia about flapping axis
I_f	- blade section moment of inertia about its elastic axis
I_k	- nondimensional gereralized mass of k bending mode
I_o	- blade section moment of inertia about its center of gravity
I_x	- nondimensional blade product of inertia about flapping and elastic axes
$M(r)$	- blade bending moment at r
M_{Af}	- blade section aerodynamic moment about elastic axis
$M_\theta, M_\theta, M_\beta$ M_β, M_g, M_g	- nondimensional aerodynamic feathering moment derivatives
$m_\theta, m_\beta, m_\beta$ $m_2, m_{g2}, m_{\theta 2}$ $m_{\theta 2}, m_{\beta 2}, m_g$ m_g	- nondimensional aerodynamic derivatives associated with blade

m - blade mass per unit length

R - blade radius

r - radial station along blade

T - blade thrust

U_p - velocity perpendicular to blade span in vertical plane at blade element

U_T - velocity perpendicular to blade span in horizontal plane at blade element

X - r/R

X_A - distance between A.C. and E.A., positive forward

X_I - distance between C.G. and E.A., positive forward

z - vertical displacement of E.A. of blade element from horizontal

β - displacement of blade, rigid flapping mode

γ - Locke number $\frac{\rho a c R^4}{I_b}$

$\eta_k(r)$ - mode shape of blade k bending mode

θ - blade pitch

ν - nondimensional root of bending-torsion characteristic equation

ν_k - nondimensional rotating, natural frequency of k bending mode

ρ - air density

ω_k - rotating natural frequency of k bending mode

ω_0 - nonrotating natural frequency of blade torsional motion

SUMMARY AND INTRODUCTON

This report presents the results of a theoretical approach to the analysis of the flutter of extremely flexible, helicopter rotor blades. The research was initiated by the fact that during experiments conducted at the United States Naval Academy, 1969-1970, it was found that there were no theoretical or experimental valves available for comparison. Some research had been done in the derivation of equations of motion for a flexible rotor blade, but actual numerical calculations had not been made. With this in mind, the equations of motion, incorporating three degrees of freedom, were derived for a rotating, flexible rotor blade. The three degrees of freedom used were pitching, flapping and the first elastic mode of flap-bending. The equations were then expanded into the characteristic equation. The objective of the report is to analyze the effect of the modulus of elasticity upon the flutter boundaries of a rotor blade. Also, at each modulus of elasticity, it is desired to study the effects of the movement of the aerodynamic center and the center of gravity upon the flutter boundary.

The area of work is done entirely in the field of classical flutter. It is assumed that the inflow of the blade is not stalled. Hence, there is no wake or stall flutter to consider.

The theoretical results consist primarily of stability plots made for each different modulus of elasticity. These plots are arrived at through the use of Routh's criteria. All of the results obtained are in very close agreement with personal observations made by the author of experiments conducted at the United States Naval Academy (Reference (23)). They also agree with observations made by the Martin Company (Reference (12)). However, the results do vary somewhat from what previous research has shown to be true for fairly rigid

blades, thus implying that more work should be done in the area of extremely flexible rotor blades.

DERIVATION OF EQUATIONS OF MOTION

Since, in this report, it was desired to study the effects of modulus of elasticity on a rotating helicopter blade, it was necessary to derive equations of motion which would incorporate this as a variable. This necessitated having the equations being of more than two degrees of freedom in order to incorporate the bending effects of the blade. Three degrees of freedom were considered; the first torsional mode, the zeroth flapping mode, and the first elastic mode of flap-bending. The two flapping, modes are illustrated in Figure 23. Ideally, of course, an infinite number of degrees of freedom should be used for the analysis, but the mathematics become impossible to handle as can be seen in Reference (1), which only used ten degrees of freedom. Also, it was decided to use only three degrees of freedom because it was felt that these were the ones which have the primary effect on blade motion.

The method of the derivation of the equations of motion vary from reference to reference. For example, References (2), (21), and (11) use LaGranges method for the derivation, whereas References (15) and (5) used the virtual work method. However, the method used in this report follows that of References (18) and (13) and is the summation of forces or moments.

Prior to the derivation a number of assumptions concerning the rotor blade were made. They are:

(1) The rotor blade is untwisted.

(2) Only the first torsional mode is considered.

(3) The rotor blade is untapered.

(4) The rotor blade is flexible, or in other words, the first elastic mode is considered.

(5) The rotor blade is of a uniform mass distribution.

(6) The rotor blade is hinged at the root, or is articulated, with no hinge offset.

Further assumptions, as needed, will be made as the derivation progresses.

First, consider Figure 1, which shows the bending out of the plane of rotation of a flexible rotor blade. The positive direction for "z" will be taken as a bending of the blade upward. It is evident that the bending moment at r due to the forces at s will be

$$M(r) = \int_r^R \left[\frac{dT(s)}{ds} - \ddot{z}(s)\, m(s)\right][s-r]\, ds - \int_r^R s\,\Omega^2 m(s)\,[z(s)-z(r)]\, ds \tag{1}$$

To arrive at the differential equation for beam bending, equation (1) must be differentiated twice with respect to r, which yields

$$\frac{d^2M(r)}{dr^2} = \frac{dT(r)}{dr} - m(r)\,\ddot{z}(r) + \frac{d^2z(r)}{dr^2}\int_r^R s\,\Omega^2 m(s)\, ds - \frac{dz(r)}{dr}\, r\,\Omega^2 m(r) \tag{2}$$

and from beam theory

$$M(r) = EI(r)\,\frac{d^2z}{dr^2}$$

Therefore, the differential equation for a blade bending out of the plane of rotation in a centrifugal force field is, after rearrangement

$$\frac{d^2}{dr^2}\left[EI(r)\frac{d^2z}{dr^2}\right] - \frac{d^2z}{dr^2}\int_r^R m s \Omega^2 dS$$

$$+ r\Omega^2 m \frac{dz}{dr} + m\ddot{z} = \frac{dT}{dr} \tag{3}$$

The form that equation (3) is in does not lend itself to a flutter analysis. Hence, with this in mind, a series solution, written in terms of normal bending modes was assumed:

$$z = \sum_{k=1}^{\infty} \eta_k(r) q_k(t) \tag{4}$$

For the moment, assume that the aerodynamic damping is zero -- i.e. $dT(r)/dr = 0$. Then, substituting equation (4) into equation (3) the bending equation becomes

$$\sum_{k=1}^{\infty} \left\{ \left[\frac{d^2}{dr^2}\left(EI\frac{d^2\eta_k}{dr^2}\right) - \frac{d^2\eta_k}{dr^2}\int_r^R m s \Omega^2 dS \right.\right.$$

$$\left.\left. + r m \Omega^2 \frac{d\eta_k}{dr}\right] q_k + m\eta_k \ddot{q}_k \right\} = 0 \tag{5}$$

assume that the motion is simple harmonic at the k rotating, undamped natual bending frequency. Therefore:

$$q_k = \bar{q}_k e^{i\nu_k \Omega t}$$

$$\ddot{g}_k = -\nu_k^2 \Omega^2 \bar{g}_k e^{i\nu_k \Omega t} = -\nu_k^2 \Omega^2 g_k$$

hence $\left[\quad\right] g_k = \nu_k^2 \Omega^2 m \eta_k g_k$

Now, putting the aerodynamic damping back into the equation, and with the above assumption, the bending equation of motion becomes

$$\sum_{k=1}^{\infty} m \nu_k^2 \Omega^2 \eta_k g_k + \sum_{k=1}^{\infty} m \eta_k \ddot{g}_k = \frac{dT}{dr} \tag{6}$$

It is now necessary to consider the effect of torsional motion upon the bending equation. There is an inertial term and a centrifugal force term due to the torsional motion which causes the coupled blade bending - torsion equation of motion to be

$$\sum_{k=1}^{\infty} m \eta_k \ddot{g}_k + \sum_{k=1}^{\infty} m \nu_k^2 \Omega^2 \eta_k g_k - m x_I \ddot{\theta} - m x_I \Omega^2 \theta = \frac{dT}{dr} \tag{7}$$

multiplying by η_k and integrating from 0 to R we get

$$M_k \ddot{g}_k + M_k \nu_k^2 \Omega^2 g_k - (\ddot{\theta} + \Omega^2 \theta) \int_0^R m \eta_k x_I \, dr = \int_0^R \eta_k \frac{dT}{dr} \, dr \tag{8}$$

where $M_k = \int_0^R m \eta_k^2 \, dr \qquad k = 1, 2, \cdots \infty$

The value of k is dependent upon the number of modes of bending chosen. In this report k = 2 since the rigid flapping and the first elastic mode are the two modes of bending being considered.

It will be assumed that the bending motion can be described by

$$z = r\beta + \eta g \tag{9}$$

where r = rigid flapping mode

η = first elastic mode

By substituting (9) into (8) and nondimensionalizing the resulting two equations by dividing by $I_b\Omega^2$ we get

$$\frac{\ddot{\beta}}{\Omega^2} + \beta - I_{\gamma}\frac{\ddot{\theta}}{\Omega^2} - I_{\gamma}\theta = \frac{1}{I_b\Omega^2}\int_0^R r\frac{dT}{dr}\,dr \tag{10}$$

$$I_2\frac{\ddot{g}}{\Omega^2} + I_2\nu_2^2 g - I_{\gamma 2}\frac{\ddot{\theta}}{\Omega^2} - I_{\gamma 2}\theta = \frac{1}{I_b\Omega^2}\int_0^R \eta\frac{dT}{dr}\,dr \tag{11}$$

where $I_b = M_1$

$$I_2 = \frac{M_2}{I_b}$$

$$I_{\gamma k} = \frac{1}{I_b}\int_0^R m\eta_k\gamma_I\,dr$$

and also, the nondimensional rotating natural frequency of the rigid flapping mode, ν_1, is equal to 1.0.

Equations (10) and (11) are the two bending equations of motion for a rotating, flexible rotor blade.

Next, the blade torsional equation of motion must be derived. Figure 2 shows the torsional geometry used. It can be seen, from the figure, that the positive direction for "θ" has been chosen as a pitch

down of the blade.

Taking moments about the elastic axis

$$-\int_o^R m(\ddot{z} - x_I\ddot{\theta})x_I\,dr + \int_o^R I_o\ddot{\theta}\,dr + \int_o^R I_o\Omega^2\theta\,dr$$

$$+ I_f\omega_o^2\theta - \int_o^R r\,m\Omega^2\frac{dz}{dr}x_I\,dr - \int_o^R m x_I\Omega^2\left(z - r\frac{dz}{dr} - x_I\theta\right)dr \qquad (12)$$

$$= \int_o^R \frac{dM_{Af}}{dr}\,dr$$

substituting for z and nondimensionalizing by $I_b\Omega^2$ we get

$$I\frac{\ddot{\theta}}{\Omega^2} + I\left[1 + \left(\frac{\omega_o}{\Omega}\right)^2\right]\theta - I_{x\beta}\beta - I_{x2}\frac{\ddot{q}}{\Omega^2}$$

$$-I_{x2}q = \frac{1}{I_b\Omega^2}\int_o^R \frac{dM_{Af}}{dr}\,dr \qquad (13)$$

where $I = \frac{1}{I_b}\left[\int_o^R m x_I^2\,dr + \int_o^R I_o\,dr\right] = \frac{I_f}{I_b}$

Equation (13), then, is the torsional equation of motion for a rotating, flexible rotor blade.

It is now necessary that the aerodynamic terms of equations (10), (11), and (13) be expanded. From Reference (3), page 272, for a unit span of a thin airfoil oscillating in an incompressible flow we have

$$\frac{dI}{dr} = -\frac{1}{8}\rho a c^2\left[\ddot{z} + U_T\dot{\theta} - (x_A - .25c)\ddot{\theta}\right]$$

$$-\frac{1}{2}\rho a c U_T C'(k)\left[U_p + U_T\theta + (.5c - x_A)\dot{\theta}\right] \qquad (14)$$

and $$\frac{dM_{Af}}{dr} = \frac{1}{8}\rho a c^2\left[(X_A - .25C)\ddot{Z} - U_T\dot{\theta}(.5C - X_A)\right.$$

$$\left. - \frac{c^2}{32}\dot{\theta} - (X_A - .25C)^2\ddot{\theta}\right] + \frac{1}{2}\rho a c U_T X_A C'(k)\cdot \qquad (15)$$

$$\left[U_p + U_T\theta + (.5C - X_A)\dot{\theta}\right]$$

where

$$U_T = \Omega r + \mu\Omega R \sin\Psi$$

$$U_p = \dot{Z} + \mu\Omega R\frac{dZ}{dr}\cos\Psi$$

The term, C'(k), is a modified Theodorsen function (see Reference (16)). It has been modified to take into account the wake effect of the rotating rotor blade. In this report, it is assumed that C'(k) has a value of one. Since this report is concerned only with the hovering case, this assumption is a very good approximation.

Normally, in this type of analysis, the mass terms which are proportional to $\ddot{z}$ and $\ddot{\theta}$ are neglected, as they shall be in this report. If it is desired, the effect of these terms can be included by the appropriate modification of the values of the blade inertial constants, but the change is usually of a negligible magnitude.

From References (18) and (21), the aerodynamic terms can be expressed as

$$\frac{I}{I_b\Omega^2}\int_0^R r\frac{dT}{dr}\,dr = -m_{\dot{\beta}}\frac{\dot{\beta}}{\Omega} - m_{\dot{q}}\frac{\dot{q}}{\Omega} - m_{\dot{\theta}}\frac{\dot{\theta}}{\Omega} \qquad (16)$$

$$- m_\theta\theta - m_\beta\beta - m_{g_2}g$$

where $m_{\dot\beta} = \frac{\gamma}{8}\,\overline{C'(k)}\left[1 + \frac{4}{3}\mu\sin\Psi\right]$

$$m_2 = \frac{\gamma}{2}\,\overline{C'(k)}\left[\int_0^1 x^2\frac{\eta}{R}\,dx + \mu\sin\Psi\int_0^1 x\frac{\eta}{R}\,dx\right]$$

$$m_{\dot\theta} = \frac{\gamma}{24}\left[1 + \frac{3}{2}\mu\sin\Psi\right]\left[\frac{c}{R} + 4\left(\frac{c}{2R} - \frac{x_A}{R}\right)\overline{C'(k)}\right]$$

$$m_\theta = \frac{\gamma}{8}\,\overline{C'(k)}\left[(1+\mu^2) + \frac{8}{3}\mu\sin\Psi - \mu^2\cos(2\Psi)\right]$$

$$m_\beta = \frac{\gamma}{2}\,\overline{C'(k)}\left[\frac{1}{3}\mu\cos\Psi + \frac{1}{4}\mu^2\sin(2\Psi)\right]$$

$$m_{g2} = \frac{\gamma}{2}\,\overline{C'(k)}\left[\mu\cos\Psi\int_0^1 x^2\frac{d}{dx}\left(\frac{\eta}{R}\right)dx + \frac{1}{2}\mu^2\sin(2\Psi)\int_0^1 x\frac{d}{dx}\left(\frac{\eta}{R}\right)dx\right]$$

also,
$$\frac{I}{I_b\Omega^2}\int_0^R \eta\frac{dT}{dr}\,dr = -m_2\frac{\dot\beta}{\Omega} - m_{\dot g}\frac{\dot g}{\Omega} - m_{\dot\theta 2}\frac{\dot\theta}{\Omega}$$

$$- m_{\theta 2}\theta - m_{\beta 2}\beta - m_g g \qquad (17)$$

where

$$m_{\dot g} = \frac{\gamma}{2}\,\overline{C'(k)}\left[\int_0^1\left(\frac{\eta}{R}\right)^2 x\,dx + \mu\sin\Psi\int_0^1\left(\frac{\eta}{R}\right)^2 dx\right.$$

$$m_{\dot\theta 2} = \frac{1}{8}\left[\mu\sin\Psi\right]\left[\frac{c}{R} + 4\left(\frac{c}{2R} - \frac{x_A}{R}\right)\overline{C'(k)}\right]\int_0^1\frac{\eta}{R}\,dx$$

$$+ \frac{\gamma}{8}\frac{c}{R}\int_0^1 x\frac{\eta}{R}\,dx + \frac{\gamma}{2}\,\overline{C'(k)}\left[\frac{c}{2R} - \frac{x_A}{R}\right]\int_0^1 x\frac{\eta}{R}\,dx$$

$$m_{\theta 2} = \frac{\gamma}{2}\,\overline{C'(k)}\left[\int_0^1\left(\frac{\eta}{R}\right)x^2 dx + \mu^2\sin^2\Psi\int_0^1\frac{\eta}{R}\,dx\right]$$

$$+ \gamma\,\overline{C'(k)}\,\mu\sin\Psi\int_0^1 x\frac{\eta}{R}\,dx$$

$$m_{\beta 2} = \frac{\gamma}{2}\,\overline{C'(k)}\left[\frac{1}{2}\mu^2\sin(2\Psi)\int_0^1\frac{\eta}{R}\,dx + \mu\cos\Psi\int_0^1 x\frac{\eta}{R}\,dx\right]$$

$$m_g = \frac{\gamma}{2}\overline{C'(k)}\left[\mu\cos\Psi\int_0^1 x\frac{\eta}{R}\frac{d}{dx}\left(\frac{\eta}{R}\right)dx + \frac{1}{2}\mu^2\sin 2\Psi\int_0^1\frac{1}{R}\frac{d}{dx}\left(\frac{\eta}{R}\right)dx\right]$$

and finally,

$$\frac{I}{I_b\Omega^2}\int_0^R\frac{dM_{Af}}{dr}\,dr = -M_{\dot\theta}\frac{\dot\theta}{\Omega} - M_{\dot\beta}\frac{\dot\beta}{\Omega} - M_{\dot g}\frac{\dot g}{\Omega}$$

$$-M_\beta\beta - M_\theta\theta - M_g g \qquad (18)$$

where

$$M_{\dot\theta} = \frac{\gamma}{8}\left[\frac{c}{R} - 4\overline{C'(k)}\frac{x_A}{R}\right]\left[\frac{c}{2R} - \frac{x_A}{R}\right]\left[\frac{1}{2} + \mu\sin\Psi\right]$$

$$M_{\dot\beta} = -\frac{\gamma}{6}\frac{x_A}{R}\overline{C'(k)}\left[1 + \frac{3}{2}\mu\sin\Psi\right]$$

$$M_{\dot g} = -\frac{\gamma}{2}\frac{x_A}{R}\overline{C'(k)}\left[\int_0^1 x\frac{\eta}{R}dx + \mu\sin\Psi\int_0^1\frac{\eta}{R}dx\right]$$

$$M_\beta = -\frac{\gamma}{4}\frac{x_A}{R}\overline{C'(k)}\left[\mu\cos\Psi + \mu^2\sin(2\Psi)\right]$$

$$M_g = -\frac{\gamma}{2}\frac{x_A}{R}\overline{C'(k)}\left[\mu\cos\Psi\int_0^1 x\frac{d}{dx}\left(\frac{\eta}{R}\right)dx + \frac{1}{2}\mu^2\sin(2\Psi)\int_0^1\frac{d}{dx}\left(\frac{\eta}{R}\right)dx\right]$$

$$M_\theta = -\frac{\gamma}{6}\frac{x_A}{R}\overline{C'(k)}\left[1 + 3\mu\sin\Psi + 3\mu^2\sin^2\Psi\right]$$

Although these aerodynamic expressions look very complicated, by assuming that the rotor is operating in the hovering state, μ equals zero. This fact greatly simplifies the above expressions. Also, if c<<R, then $M_{\dot{\theta}}$ and $M_{\dot{\theta}2}$ are normally set equal to zero.

By assuming that the advance ratio is zero, the following derivatives become zero:

$$M_\beta = 0$$

$$M_{g2} = 0$$

$$M_{\beta 2} = 0$$

$$M_g = 0$$

$$M_\beta = 0$$

$$M_g = 0$$

Hence, the final form of the equations of motion become: the flapping equation

$$\frac{\ddot{\beta}}{\Omega^2} + m_{\dot{\beta}} \frac{\dot{\beta}}{\Omega} + \beta - I_x \frac{\ddot{\theta}}{\Omega^2} + (m_\theta - I_x)\theta + m_2 \frac{\dot{q}}{\Omega} = 0 \tag{19}$$

the flap-bending equation

$$I_2 \frac{\ddot{q}}{\Omega^2} + m_{\dot{q}} \frac{\dot{q}}{\Omega} + I_2 \nu_2^2 q - I_{x2} \frac{\ddot{\theta}}{\Omega^2} + (m_{\theta 2} - I_{x2})\theta \tag{20}$$

$$+ m_2 \frac{\dot{\beta}}{\Omega} = 0$$

and the torsion equation

$$-I_x \frac{\ddot{\beta}}{\Omega^2} + M_{\dot{\beta}} \frac{\dot{\beta}}{\Omega} - I_x \beta + \bar{I} \frac{\ddot{\theta}}{\Omega^2} + M_{\dot{\theta}} \frac{\dot{\theta}}{\Omega}$$

$$+ \left[M_\theta + \bar{I} + I \left(\frac{\omega_i}{\Omega} \right)^2 \right] \theta - I_{x2} \frac{\ddot{q}}{\Omega^2} + M_{\dot{q}} \frac{\dot{q}}{\Omega} - I_{x2}\, q = 0 \qquad (21)$$

This concludes the derivation of the equations of motion for a flexible, rotating rotor blade. Appendix IV gives an explanation of the various terms in the above equations.

ANALYSIS OF EQUATIONS OF MOTION

There are a couple of ways in which the equations of motion can be analyzed in order to obtain the flutter boundaries. By one method, the equations of motion have to be solved for the critical flutter frequency and the RPM at which the flutter instability begins. This is a very good approach to the problem as long as there are no more than two degrees of freedom. As soon as the system is increased by even only one degree of freedom, the mathematics involved in the solution become unmanageable, without the aid of a lot of computer time. Due to the time restriction placed on this report this method was ruled out as just being too time consuming. If there is interest in this approach, References (8) and (19) would be of great advantage.

A second, much simpler method of obtaining the flutter boundaries is to use Routh's Criteria. This, as in the first method, also requires that the characteristic equation be obtained. However, a solution of the equation is not needed. According to Routh, for a system to be dynamically stable it is necessary that all the coefficients of the characteristic equation be of the same sign. Also, at the same time, it is necessary that Routh's discriminant also be positive. This discriminant is obtained from an array. The development of this array and the discriminants is shown in Appendix II.

Now that the method of analysis is known, the equations of motion must be put in the correct form. In other words, the characteristic equation of motion has to be obtained. Before this is done, though, it should be pointed out that there are no time-dependent terms in the equations of motion. This is because the hovering condition has been assumed and hence

the advance ratio is zero which eliminates the time-dependent terms. This means that all of coefficients of the characteristic equation will be constant, and that a conventional technique for an explicit solution of the equation could be used if so desired. Even though solution was not attempted, having constant coefficients simplified the analysis.

To further simplify the analysis, it was assumed that the motion of the blade was a simple harmonic motion. Therefore, it was known that the harmonic perturbations of the variables β, θ, and g would be of the following form:

$$\beta = \beta_0 e^{\nu\Omega t} \tag{22}$$

$$g = g_0 e^{\nu\Omega t} \tag{23}$$

$$\theta = \theta_0 e^{\nu\Omega t} \tag{24}$$

Substituting (22), (23), and (24) into (19), (20), and (21), and after dividing all the equations by $e^{\nu\Omega t}$, the equations of motion become:

the flapping equation

$$\beta_0 \nu^2 + m_\beta \beta_0 \nu + \beta_0 - I_X \theta_0 \nu^2 + (m_\theta - I_X)\theta_0 + m_2 g_0 \nu = 0 \tag{25}$$

the flap - bending equation

$$I_2 g_0 \nu^2 + m_{\dot{g}} g_0 \nu + I_2 \nu_2^2 g_0 - I_{X2} \theta_0 \nu_2^2 + (m_{\theta 2} - I_{X2})\theta_0 + m_2 \beta_0 \nu = 0 \tag{26}$$

and the torsion equation

$$-I_x \beta_o \nu^2 + M_{\dot{\beta}} \beta_o \nu - I_x \beta_o + I \theta_o \nu^2 + M_{\dot{\theta}} \theta_o \nu$$
$$+ \left[M_\theta + I + I\left(\frac{\omega_o}{\Omega}\right)^2 \right] \theta_o - I_{xz} g_o \nu^2 + M_{\dot{q}} g_o \nu - I_{xz} g_o = 0 \qquad (27)$$

It can be seen that now all three equations are in terms of ν, which is a non-dimensional root.

$$\nu = \frac{\omega}{\Omega}$$

If the equations were solved for ν, the answer would be the critical, reduced frequency for flutter. Since the equation was not to be solved another parameter had to be chosen for the stability plots. This was the nonrotating, reduced torsional frequency, ω_o/Ω.

The equations can now be put into a determinant form, and the determinant expanded to arrive at the characteristic equation. This also shows why more than a few degrees of freedom are not very often analyzed. With three degrees of freedom the determinant is a 3 X 3, and the expansion is fairly complicated. As the degrees of freedom are increased the square determinant increases by one and becomes more and more difficult to expand. The full expansion of the determinant used in this report may be found in Appendix I. A quick look at Appendix I will show how unwieldy the coefficients of the characteristic equation become, with some coefficients having as many as thirty (30) terms. Increasing the system by only one degree of freedom nearly doubles the number of terms of the coefficients, and the complexity of the problem.

After expansion of the determinant, the characteristic equation is found to be a sixth-order equation of the following form:

$$A\nu^6 + B\nu^5 + C\nu^4 + D\nu^3 + E\nu^2 + F\nu + G = 0 \qquad (28)$$

Once the characteristic equation was derived, it was possible to calculate the coefficients for the varying parameters and to establish the flutter boundaries. The main parameter of interest was the modulus of elasticity of the rotor blade. Since the equations of motion were derived in terms of normalized mode shapes, the only place the modulus of elasticity enters the equations is through the mode shapes. Hence, it was necessary to use several different mode shapes in order to study the effect of a modulus of elasticity tending towards zero. The specific mode shapes used and why, is explained elsewhere in this report.

Besides studying the effect of the modulus of elasticity, it was also desired to study the effects of other parameters at each respective mode shape. At each mode shape, two other parameters were varied. These were the center of gravity location and the aerodynamic center location. The location of both of these axes was with respect to the elastic center axis. The center of gravity and the aerodynamic center were varied first independently and then they were varied together. All of the results were then plotted. In all the plots the ordinate is ω_o/Ω, which is the reduced, nonrotating natural frequency of blade torsional motion. By using this as a parameter it is possible to tell, for a particular torsional frequency, at what RPM the blade system becomes unstable. Also, for a particular RPM it is possible to calculate the corresponding critical nonrotating torsional frequency. The abscissa of the stability plots was either the center of gravity location or the aerodynamic center location.

Due to the complexity of the coefficients of the characteristic equation, all the numerical calculations were done on a computer. The computer used was IBM 360 Model 91. The computer was located at the Princeton University Computer Center at Princeton University. Since the program used was just a simple mathematical routine, it is not included in this report. All of the results were transferred to graphs, which are included, however.

MODE SHAPES

As has already been seen, the equations of motion of the rotating rotor blade were derived in terms of normalized mode shapes. It should also be noticed that the modulus of elasticity does not appear explicitly in the equation, but rather is incorporated into the mode shapes. This made it necessary to choose various mode shapes which would be representative of the varying modulus of elasticity. It was possible to obtain exact mode shapes for two limiting cases (see References (18) and (14)).

The two limiting cases are

(1) A rotor blade with the modulus of elasticity equal to zero.

(2) A rotor blade that is considered to be a typical rigid rotor blade.

It was not possible to find exact mode shapes for a modulus of elasticity between case (1) and case (2). However, by graphing the above two mode shapes and then drawing curves which fell between these two cases, it was possible to obtain other mode shapes. See Figure 3. Only two intermediary mode were chosen, making a total of four (4).

The reason that an infinitely stiff blade was not chosen as the limiting case was that it is nearly impossible to achieve such a situation with a long, thin rotor blade. Therefore, the mode shape of a typical rotor blade was used. Mathematically the mode shape can be expressed as:

$$\frac{\Delta}{R} = 3X - 4X^2 \tag{29}$$

This mode shape was then substituted into the nondimensional derivatives giving the following:

$$m_{\dot{\beta}} = \frac{\gamma}{8} \qquad M_{\dot{\theta}} = \frac{3\gamma}{16}\left[\frac{c}{R} - 4\frac{x_A}{R}\right]\left[\frac{c}{2R} - \frac{x_A}{R}\right]$$

$$m_z = \frac{-\gamma}{40} \qquad M_{\dot{\beta}} = 0$$

$$m_\theta = \frac{\gamma}{8} \qquad M_{\dot{\beta}} = -\frac{\gamma x_A}{6R}$$

$$m_{\dot{\beta}} = \frac{7\gamma}{120} \qquad M_\theta = -\frac{\gamma x_A}{6R}$$

$$m_{\theta z} = \frac{-\gamma}{40}$$

These derivatives were then used to calculate the coefficients of the characteristic equation.

Now look at case (1); the rotor blade with the modulus of elasticity equal to zero. The mode shape for this case was evaluated in a Ph. D. thesis written at Rensselaer Polytechnic Institute. (Reference (14)). It was found that the mode shape was of the following form:

$$\frac{\eta}{R} = \frac{\sqrt{7}}{2}\left[3x - 5x^3\right] \tag{30}$$

With this as the mode shape the non-dimensional derivatives which are affected by the mode shape now have the following values:

$$m_z = -\frac{\sqrt{7}\gamma}{48} \qquad m_{\theta z} = -\frac{\sqrt{7}\gamma}{48}$$

$$m_{\dot{\beta}} = \frac{21\gamma}{64}$$

The rest of the derivatives do not change in value.

After much drawing of curves and curve fitting, it was possible to arrive at two other mode shapes which fell between the two limiting cases. The first of these intermediary shape was of the form:

$$\frac{\eta}{R} = 3x - 5x^3 \tag{31}$$

with the corresponding derivatives having the values:

$$m_2 = \frac{-\gamma}{24}$$

$$m_{\dot{q}} = \frac{3\gamma}{16}$$

$$m_{\theta 2} = \frac{-\gamma}{24}$$

The second intermediary shape was of the form:

$$\frac{\eta}{R} = \frac{\sqrt{17}}{2}\left[3\chi - 4\chi^2\right] \tag{32}$$

and its corresponding derivatives had the values

$$m_2 = \frac{-\sqrt{17}\gamma}{80}$$

$$m_{\dot{q}} = \frac{49\gamma}{480}$$

$$m_{\theta 2} = \frac{-\sqrt{17}\gamma}{80}$$

One interesting fact discovered while arriving at the mode shapes was that ν_2, the nondimensional rotating natural frequency of the second bending mode, did not change as the modulus of elasticity changed. (see References (14) and (20)). Hence, it was possible to use the same frequency throughout all the calculations. In this case the frequency turned out to be 2.5.

The reason there is no change in the frequency is that it is more strongly dependent upon mass distribution than it is modulus of elasticity. And since all the cases in this report have the same mass distribution, i.e. uniform, the frequency of the second bending mode, or in other words, the first elastic mode, remains constant.

It should also be mentioned that the normalized mode shapes are also strongly dependent upon mass distribution. Although this fact was not considered in this report, it would be worthwhile to do so.

RESULTS

Overall Results

As we previously mentioned, the coefficients of the characteristic equation and the values of Routh's discriminants were all calculated; and then, using Routh's criteria, the flutter boundaries were plotted. For all the calculations, one rotor blade type was used. The rotor blade used was a model rotor blade developed by Cornell Aeronautical Laboratories for some of their experiments. (see References (6) and (5)). The representative data for this model blade is given in Appendix III.

For each mode shape, four different situations were analyzed in order to provide a complete flutter analysis of the rotor blade for the parameters involved. The cases investigated were:

(1) The aerodynamic center and the center of gravity were coincident with the elastic axis.

(2) The aerodynamic center was coincident with the elastic axis, and the center of gravity was varied in location forward and aft of the elastic axis.

(3) The center of gravity was coincident with the elastic axis, and the aerodynamic center was varied in location forward and aft of the elastic axis.

(4) And finally, both the center of gravity and the aerodynamic center were varied in location forward and aft of the elastic axis.

Each case shall be discussed separately, and then, an overall analysis shall be given.

First, let's consider case (1), where all three axes are coincident. It was not possible to plot a graph of the dynamic stability of this system

in a manner which could easily be understood. Therefore, the results were put in table form and are shown in Table 1. In the table, the mode shapes are numbered 1 through 4, with mode shape number 1 being the most rigid case and mode shape number 4 being the most flexible case. The first thing that will be noticed is that as the modulus of elasticity is decreased (the blade becomes more flexible) the RPM at which the rotor blade becomes unstable is decreased (an increase in ω_o/Ω is a decrease in RPM).

From Reference (22) it was found that a typical operating value for ω_o/Ω is 8.0. Hence, it immediately becomes evident, that with an extremely flexible rotor blade the blade would always be just on the verge of instability, requiring only a slight abnormal operating condition to cause an unstable flutter. To make matters even worse, there were some observations made by the Martin Company, of extremely flexible blades (Reference (12)) which showed that as the modulus of elasticity of a rotor blade is decreased, the nonrotating natural frequency of the blade torsional motion, ω_o, also decreases. This means that ω_o/Ω will also be reduced and hence, the stability margin is decreased. All of this points to the problems designers have with extremely flexible rotor blades.

In the second case, the aerodynamic center and the elastic axis were coincident. The results are shown in Figure 4. Once again it was observed that as the modulus of elasticity was decreased, the region of instability was increased. It can be seen that there was a gradual increase in instability for all mode shapes as the center of gravity was displaced further and further from the elastic axis. However, when the center of gravity was located more than 20% chord from the elastic axis the system

became unstable for all values of $\frac{\omega_0}{\Omega}$ analyzed. Other References do not show this marked instability due to the fact that in the majority of the analyses the center of gravity is not moved as far as 20% chord away from the elastic axis. The reason for this sharp instability is discussed elsewhere in this report.

In case (3), the center of gravity was coincident with the elastic axis. This says that the rotor blade was mass balanced. Again it was observed that a reduction in the stiffness of a rotor blade increases the region of instability. It was also found that as the aerodynamic center was moved aft of the elastic axis, the flutter boundary began to fall off, whereas if it was moved forward of the elastic axis a plateau for the flutter boundary was reached. See Figure 5. This would suggest that it is preferable to have the aerodynamic center aft of the elastic axis. That is the same conclusion reached by Goldman in Reference (12). Contrary to case (2), and as will presently be seen, case (4), case (3) does not have the sharp upward break in the flutter boundary. As might be suspected, this was because the rotor blade was mass balanced.

Figures 6-19 show the final results of case (4), in which both the center of gravity and the aerodynamic center were varied. As was expected, it was found that in this case, also, that reducing the stiffness of a blade increased the instability. It was further found, again, that it was preferable to have the aerodynamic center located aft of the elastic axis. (see Figure 20). This was the same conclusion reached when case (3) was analyzed. Case (4) also illustrated the same strange break in the flutter boundary that was found in case (2). For some reason there appeared to be a limiting center of gravity position, beyond which the system was unstable

for all values of ω_0/Ω.

Since an optimum positon for the aerodynamic center had been found, it was deemed desirable to also find an optimum position for the center of gravity. With this in mind, Figure 21 was drawn. From this figure it can be seen that the region of instability will be the smallest when the center of gravity is coincident with the elastic axis. By looking at the equations of motion it can be seen that in this situation the torsional flutter is uncoupled from the flapping and flap-bending flutter. (see Reference (19)). As soon as the rotor blade is no longer mass balanced the pitching and the flapping of the rotor blade become coupled and the instability is increased. It was also observed that a forward center of gravity movement was preferred over a rearward movement. This fact is further supported by observations made by Goldman in Reference (12).

In no other references is there any mention of forward center of gravity movement made. And if the rotor blade is fairly rigid there is no real reason to consider this fact. However, if a rotor blade being designed is extremely flexible, the center of gravity location could be the source of many problems.

From personal observations made by the author of some experiments conducted at the United States Naval Academy with extremely flexible blades, Reference (23), the critical importance of center of gravity location was seen. The rotor blades used had originally been constructed with the idea of having the center of gravity and the elastic axis coincident. However, it was found that actually the center of gravity was aft of the elastic axis. At the time this was not of too much concern. However, upon conducting the experiments it was not possible to keep the blade stable. This theoretical analysis

for all values of ω_0/Ω.

Since an optimum positon for the aerodynamic center had been found, it was deemed desirable to also find an optimum position for the center of gravity. With this in mind, Figure 21 was drawn. From this figure it can be seen that the region of instability will be the smallest when the center of gravity is coincident with the elastic axis. By looking at the equations of motion it can be seen that in this situation the torsional flutter is uncoupled from the flapping and flap-bending flutter. (see Reference (19)). As soon as the rotor blade is no longer mass balanced the pitching and the flapping of the rotor blade become coupled and the instability is increased. It was also observed that a forward center of gravity movement was preferred over a rearward movement. This fact is further supported by observations made by Goldman in Reference (12).

In no other references is there any mention of forward center of gravity movement made. And if the rotor blade is fairly rigid there is no real reason to consider this fact. However, if a rotor blade being designed is extremely flexible, the center of gravity location could be the source of many problems.

From personal observations made by the author of some experiments conducted at the United States Naval Academy with extremely flexible blades, Reference (23), the critical importance of center of gravity location was seen. The rotor blades used had originally been constructed with the idea of having the center of gravity and the elastic axis coincident. However, it was found that actually the center of gravity was aft of the elastic axis. At the time this was not of too much concern. However, upon conducting the experiments it was not possible to keep the blade stable. This theoretical analysis

now explains why this was so. For flexible, i.e. a very small modulus of elasticity, the center of gravity should be coincident with or forward of the elastic axis.

All of the above results can be reduced down to a few certain facts that must be kept in mind when designing an extremely flexible rotor blade. Number one is that it is desirable to have the aerodynamic center aft of the elastic axis. Secondly, it was found that the center of gravity location is critical and should be conicident with or forward of the elastic axis. It was also found that as the modulus of elasticity is reduced, the nonrotating natural frequency of blade torsional motion, ω_o, becomes an important factor. The reduction of ω_o that occurs with a reduction of modulus of elasticity tends to place the operating mode of the rotor blade a lot closer to instability. This also explains why it is desirable to have the center of gravity forward of the elastic axis. The extra margin of stability that is gained is needed.

One other observation made in this analysis concerned the effect of center of gravity displacement from the elastic axis upon the torsional frequency. From the figures it can easily be seen that as the center of gravity is displaced further and further from the elastic axis, in either direction, the torsional frequency required for flutter is increased.

Flutter Phenomena

As was found in discussing the overall results, case (2) and case (4) of the analysis disclosed a very sharp upward break in the flutter boundary that occured at a center of gravity location of more than 20% chord displacement from the elastic axis. Since this break in the flutter curve occured within one chord length it was considered necessary to analyze it

and see if the reason for its occurrence could be discovered. First, it was important to find out whether it was the coefficients of the characteristic equation or one of Routh's discriminants which was displaying the instability.

After going back over all of the data, it was found that in all instances it was the coefficients of the characteristic equation which were displaying the instability. Also, it was observed that it was only the coefficients of the two highest order terms, or in other words the "A" coefficient and the "B" coefficient if the equation is written in the form of Equation (28). The next step in the analysis was then to find out which term of the coefficient caused the instability, or speaking mathematically, which term caused the coefficient to become negative.

The two coefficients may be expressed as follows:

$$A = I I_2 - I_{x2}^2 - I_x^2 I_2 \tag{33}$$

$$B = 2 I_x I_{x2} m_2 + I_x I_2 M_{\dot{\beta}} - I_x^2 m_{\dot{q}} + I_x M_{\dot{q}} + I_2 M_{\dot{\theta}}$$

$$+ I m_{\dot{q}} - I_{x2}^2 m_{\dot{\beta}} + I I_2 m_{\dot{\beta}} \tag{34}$$

Although all cases were analyzed, the case that will be discussed in this report will be the case where the modulus of elasticity equals zero. The results are the same for the rest of the cases, but with a little different numbers for the coefficients.

Using the derivatives for the case of zero modulus of elasticity, and substituting in the corresponding numbers, the coefficients may now be written in the following form:

$$A = .000287 - .0156 X_I^2 - .0844 X_I^2 \tag{35}$$

$$B = -.013 X_I^2 + .023 X_I X_A - .113 X_I^2 + .0007 - .015 X_A$$
$$+ .069 X_A^2 + .000386 - .043 X_I^2 + .000087 \quad (36)$$

Let's consider the "A" coefficient first. A look at the numerical equation shows that it will be due to the second and third terms that the equation first becomes negative and hence the system becomes unstable. These two terms, which are dependent upon center of gravity position, are I_x and I_{x2}. Both of these terms are the nondimensional blade product of inertia about the flapping and elastic hinges. Going back to the original equations of motion, it was found that it was the inertial moments about the pitching and flapping axes which gave rise to the above terms. These terms are also called the mass unbalance terms since if the rotor blade is mass balanced they are zero.

Now let's look at the "B" coefficient. It can be seen that this coefficient is dependent upon both center of gravity position and aerodynamic center position. However, it was found that the only time that the "B" coefficient was important was when the aerodynamic center was aft of the elastic axis and the center of gravity forward. This meant that the secomd term was the most important term. It was also found that I_x had the primary effect, as it did in the "A" coefficient.

As can be seen, in all cases the sharp break in the flutter curve was due to the mass unbalance terms, I_x and I_{x2}. From looking at the equations of motion it can be seen that the instability occurs due to a coupling of the inertias between the pitching and flapping of the rotor blade. Also, it should be mentioned that these two inertia moments arise due to either a pitching acceleration or a flapping acceleration.

That, then, explains the reason for the sharp upward break in the

All this shows that a divergent instability becomes of no more importance for an extremely flexible blade than it was for a fairly rigid rotor blade.

CONCLUSIONS

Based on the theoretical results previously discussed, the following basic conclusions were reached.

1. As the modulus of elasticity of a rotor blade is decreased the region of instability increases. Since, at the same time, ω_o is decreasing there can be a very real problem with the dynamic stability of an extremely flexible rotor blade.

2. In the design of an extremely flexible rotor blade, it is desirable to have the aerodynamic center located aft of the elastic axis in order to obtain dynamic stability.

3. Also, when designing an extremely flexible rotor blade it is necessary to have the center of gravity coincident with the elastic axis or forward of it. This is contrary to classical flutter analysis, but is a necessary condition if the blade is to be extremely flexible, due to the decrease in ω_o.

4. Coupling of the mass unbalance terms, or in other words, the inertial effects due to pitching and flapping acceleration causes a sharp upward break in the flutter boundary if the center of gravity is displaced more than 20% chord away from the elastic axis. This occurs whether the center of gravity is forward or aft of the elastic axis.

5. A change in the modulus of elasticity of a rotor blade has no effect on the divergence boundary of the blade.

RECOMMENDATIONS

Due to the time restriction on this report there were many areas of the flutter problem that the author was not able to look into. With this in mind, the following are several recommendations for future study in this field.

1. Since this report was strictly theoretical, an experimental analysis should be made to verify the results obtained herein.

2. It would be informative to do both theoretical and experimental research on the effect of extremely flexible blades upon forward flight.

3. Although this report only considered classical futter, the other two types of flutter - wake flutter and stall flutter - should certainly be looked at.

4. One thing that probably will be a big factor in the construction of extremely flexible rotor blades is a tip mass. Therefore, the effect of a tip mass upon the flutter boundaries of a rotor blade is in itself a big subject to consider. Also, a mass distribution, other than uniform might be considered.

REFERENCES

1. P. J. Arcidiacono: "Prediction of Rotor Instability at High Forward Speeds", USAAVLABS Technical Report 68-18A, Vol. I, February 1969.
2. C. J. Astill, C. F. Niebanck: "Prediction of Rotor Instability at High Forward Speeds", USAAVLABS Technical Report 68-18B, Vol. II, February 1969.
3. R. L. Bisplinghoff, H. Ashley, R. L. Halfman: Aeroelasticity, Addison-Wesley Publishing Company, Inc., Reading, Massachusetts, 1955.
4. G. W. Brooks, J. E. Baker: "An Experimental Investigation of the Effect of Various Parameters Including Tip Mach Number on the Flutter of Some Model Helicopter Rotor Blades", NACA TN 4005, September 1958.
5. T. T. Chang: "A Flutter Theory for a Flexible Helicopter Rotor Blade in Vertical Flight", Cornell Aero Lab Report No. SB-862-S-1, July 1954.
6. H. Doughaday, F. DuWaldt, C. Gates: "Investigation of Helicopter Rotor Flutter and Load Amplification Problems", Cornell Aero Lab Report No. SB-862-S-4, August 1956.
7. F. A. DuWaldt, C. A. Gates, R. A. Piziali: "Investigation of the Flutter of a Model Helicopter Rotor Blade in Forward Flight", WADD Technical Report 60-479, July 1960.
8. F. A. DuWaldt, C. A. Gates, R. A. Piziali: "Investigation of Helicopter Rotor Blade Flutter and Flapwise Bending Response in Hovering", WADC Technical Report 59-403, August 1959.
9. F. DuWaldt, C. Gates: "An Experimental and Theoretical Study of the Low Frequency Flapping-Pitching Flutter of a Hovering Rotor

Blade", Cornell Aero Lab Report No. SB-680-S-2, September 1952.

10. G. Flicker: "The Flutter of Helicopter Blades", Air Materiel Command Report No. F-TR-1177-ND, July 1948.
11. L. Goland, A. A. Perlmutter: "A Comparison of the Calculated and Observed Flutter Characteristics of a Helicopter Rotor Blade Having Both Control System and Blade Flexibility", Princeton Report No. 333, December 1955.
12. R. L. Goldman: "Some Observations on the Dynamic Behavior of Extremely Flexible Rotor Blades", IAS Paper No. 60-44, January 1960.
13. P. de Guillenchmidt: "Calculation of the Bending Stresses in Helicopter Rotor Blades", NACA TM 1312, March 1951.
14. D. S. Jenny: "On the Behavior of Extremely Flexible Rotating Beams", Ph.D. Thesis, Rensselaer Polytechnic Institute, April 1968.
15. A. Z. Lemnios, A. F. Smith, A. Berman: "The Aeroelastic Behavior of Rotary Wings in Forward Flight", Kaman Aircraft Corporation Report No. R-585, Vol. I.
16. R. G. Loewy: "A Two-Dimensional Approximation to the Unsteady Aerodynamics of Rotary Wings", Cornell Aero Lab Report No. 75, October 1955.
17. R. G. Loewy: "Review of Rotary-Wing V/STOL Dynamics and Aeroelastic Problems", AIAA Paper No. 69-202, February 1969.
18. R. H. Miller, C. W. Ellis: "Helicopter Blade Vibration and Flutter", Journal of American Helicopter Society, Vol. 1, No. 3, July 1956.
19. M. Morduchow: "A Theoretical Analysis of Elastic Vibrations of Fixed-Ended and Hinged Helicopter Blades in Hovering and Vertical Flight", NACA TN 1999, January 1950.

20. Norwegian Institute of Technology: "Rotor Blade Vibration Modes and Frequencies", ASTIA No. AD-410217, December 1962.

21. A. A. Perlmutter: "The Effects of a Spanwise Variation of the Section Shear Center Position on the Flutter Characteristics of a Helicopter Blade", Princeton Report No. 350, May 1956.

22. K. W. Shipman, E. R. Wood: "A Theoretical Method for Rotor Blade Flutter in Forward Flight", American Helicopter Society Preprint No. 410, June 1970.

23. S. R. Swah: "Flyaway Seat", United States Naval Academy TSPR No. 3, May 1970.

TABLE 1. DYNAMIC STABILITY OF CASE (1)

MODE SHAPE	DYNAMIC STABILITY
1	unstable for $\omega_o/\Omega \leq 5$, stable elsewhere
2	unstable for $\omega_o/\Omega \leq 6$, stable elsewhere
3	unstable for $\omega_o/\Omega \leq 6$, stable elsewhere
4	unstable for $\omega_o/\Omega \leq 7$, stable elsewhere

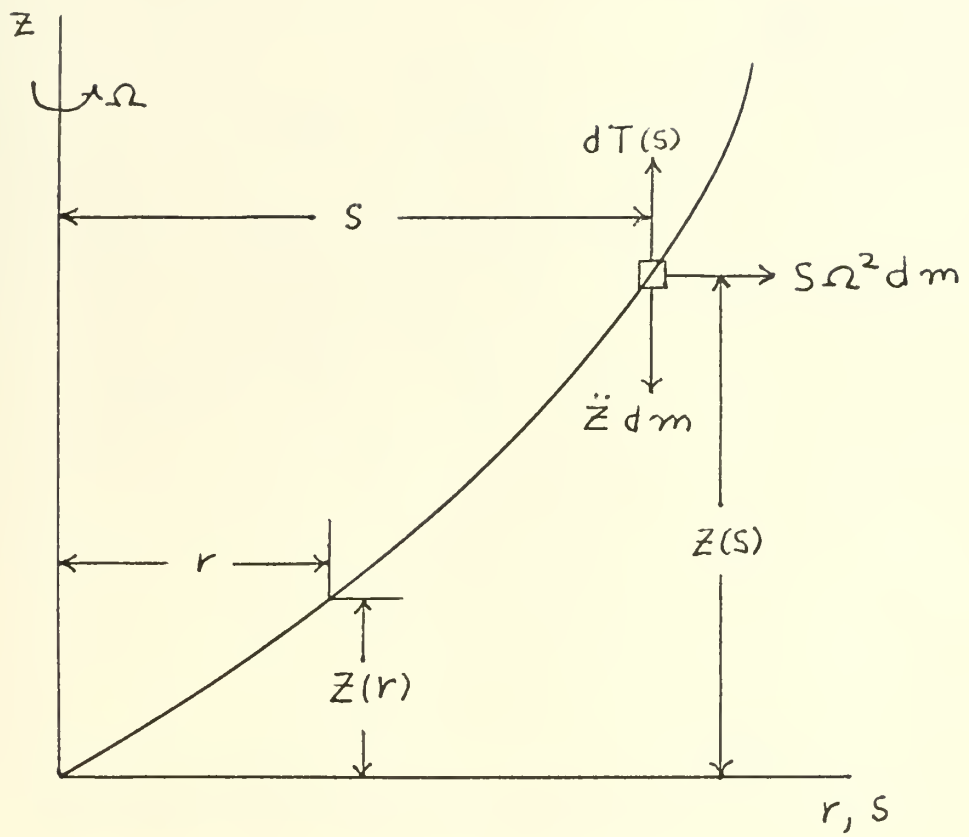

FIGURE 1. BLADE BENDING GEOMETRY

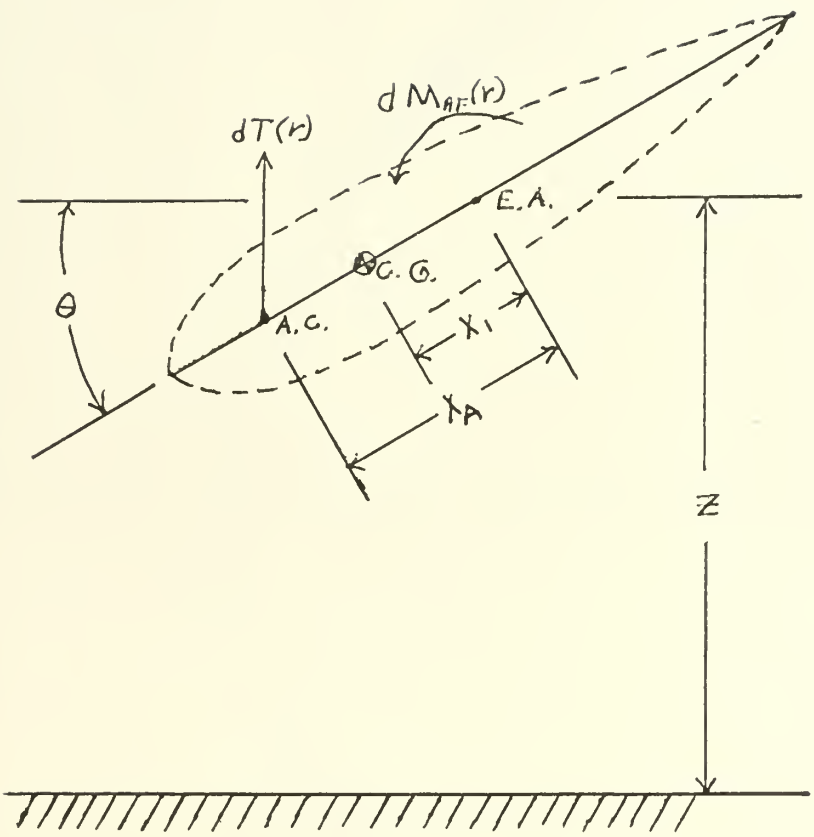

FIGURE 2. BLADE TORSIONAL GEOMETRY

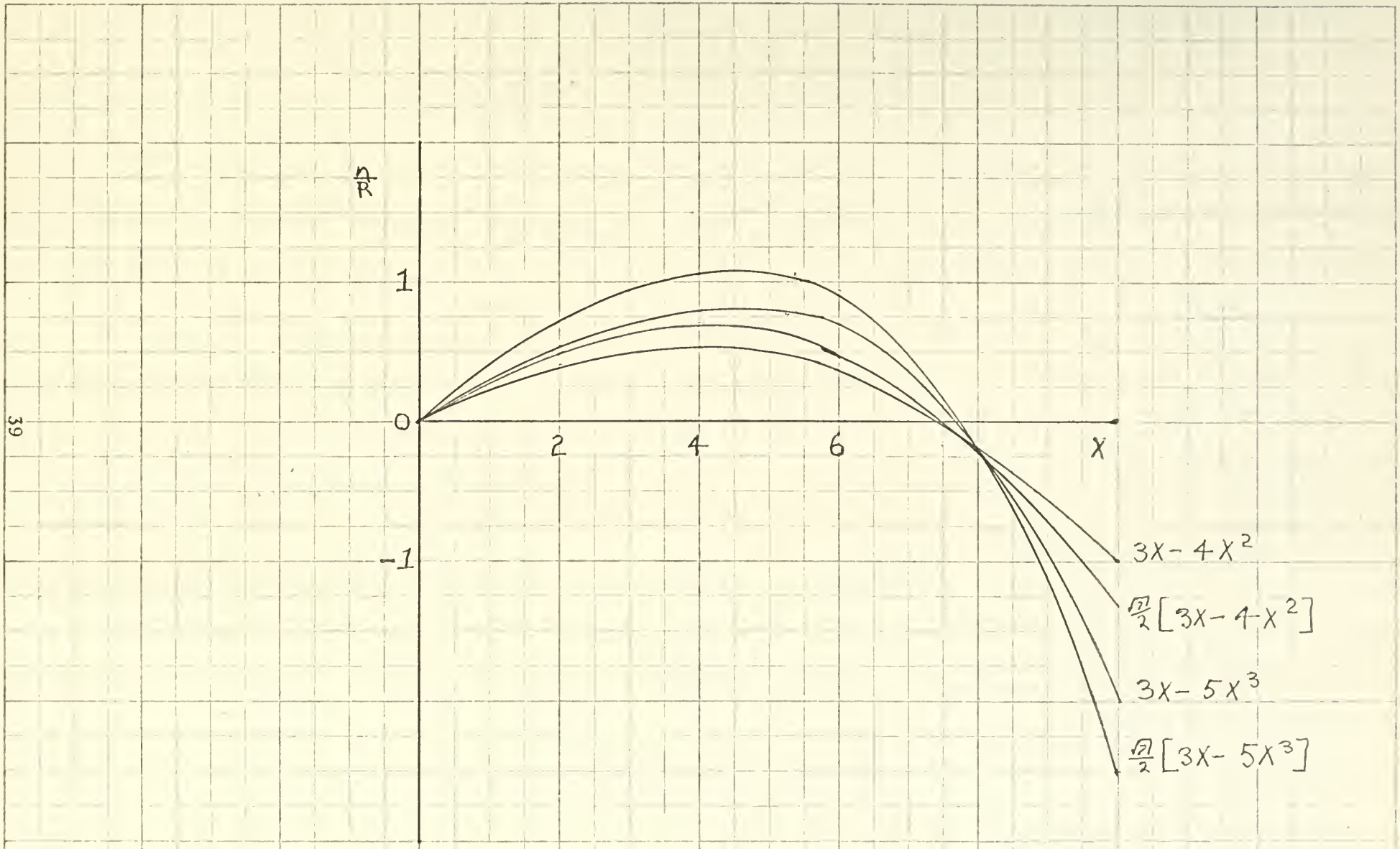

FIGURE 3. MODE SHAPES

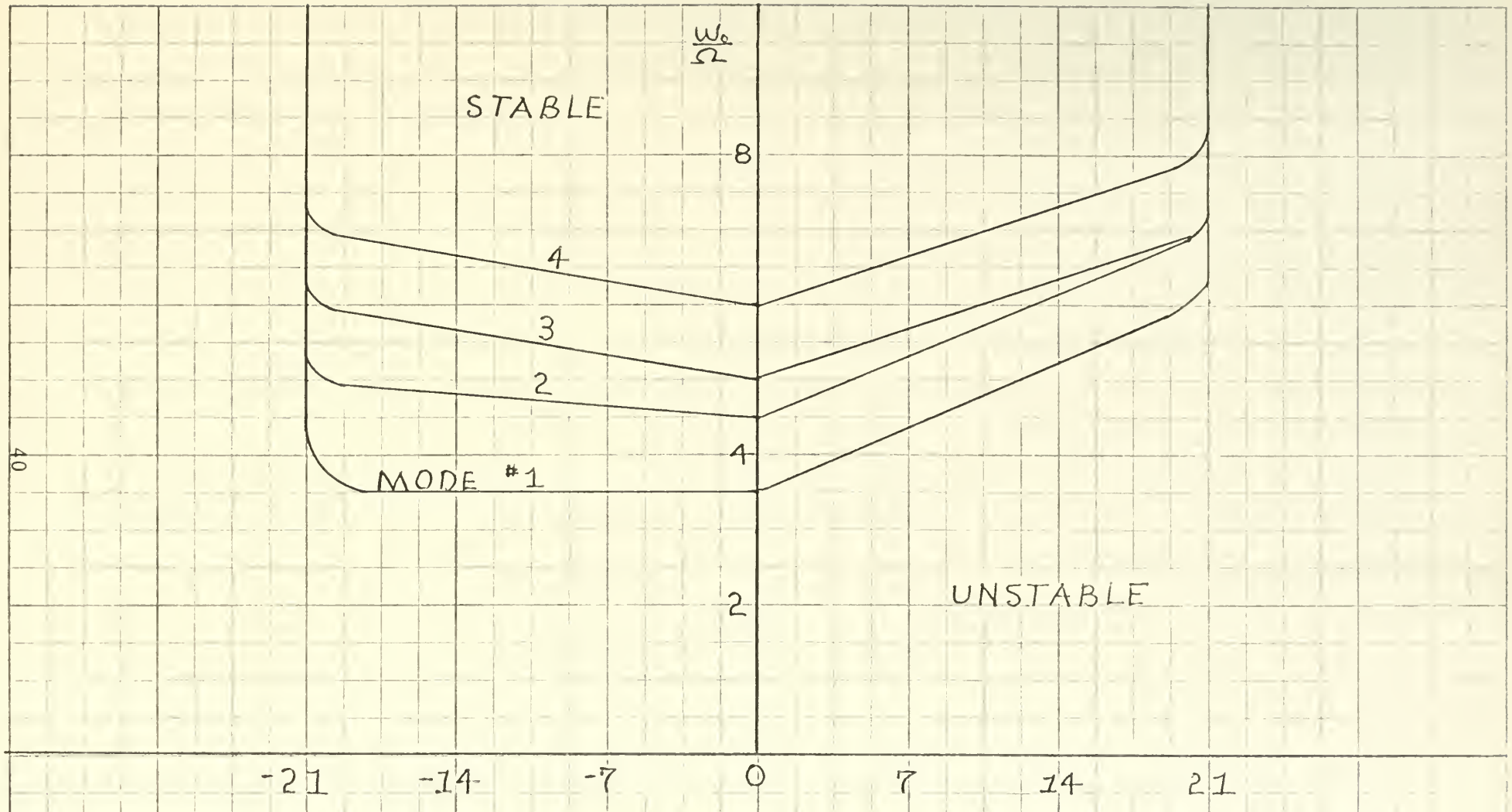

FIGURE 4. STABILITY BOUNDARIES — A.C. = E.A.

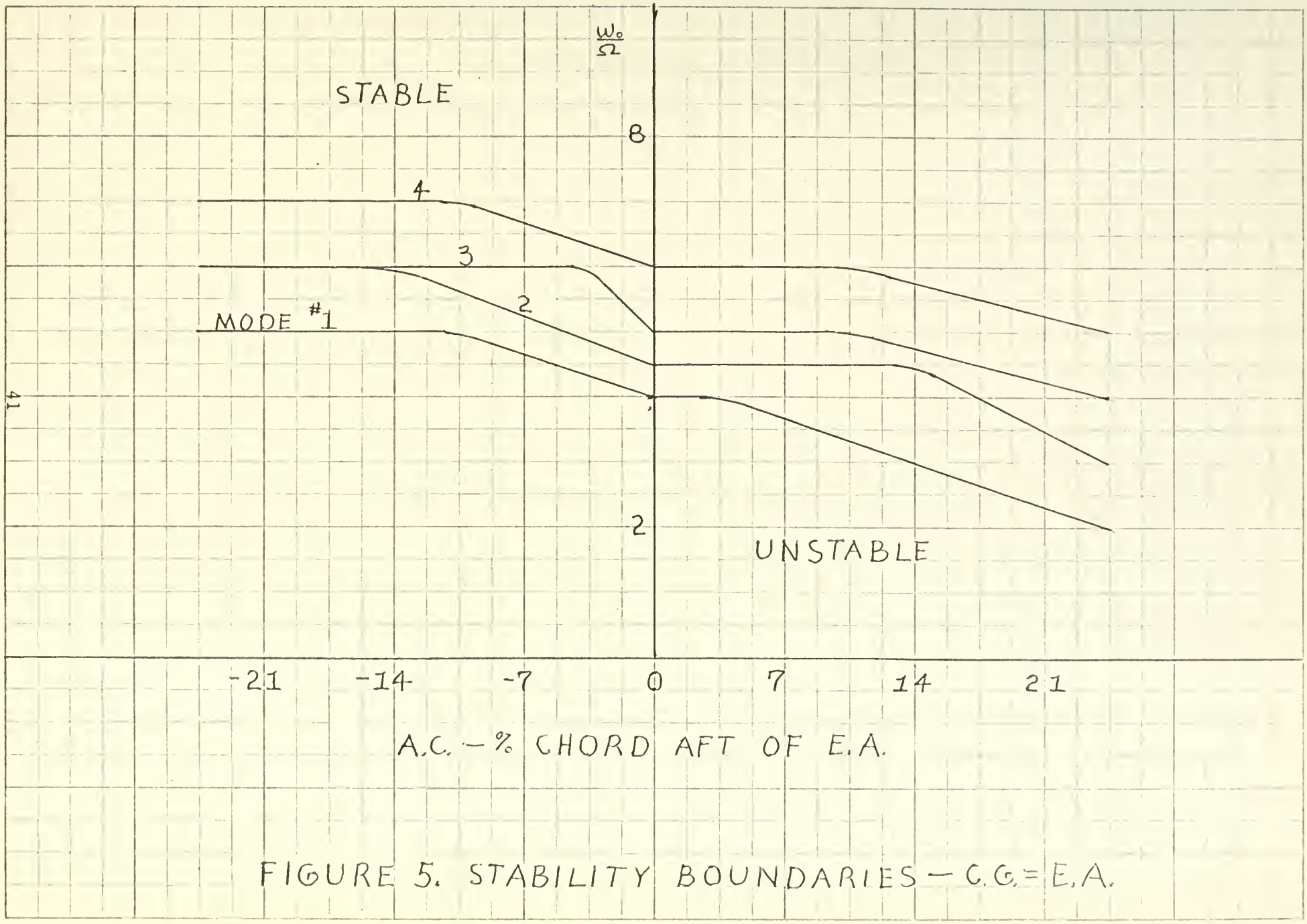

FIGURE 5. STABILITY BOUNDARIES — C.G. = E.A.

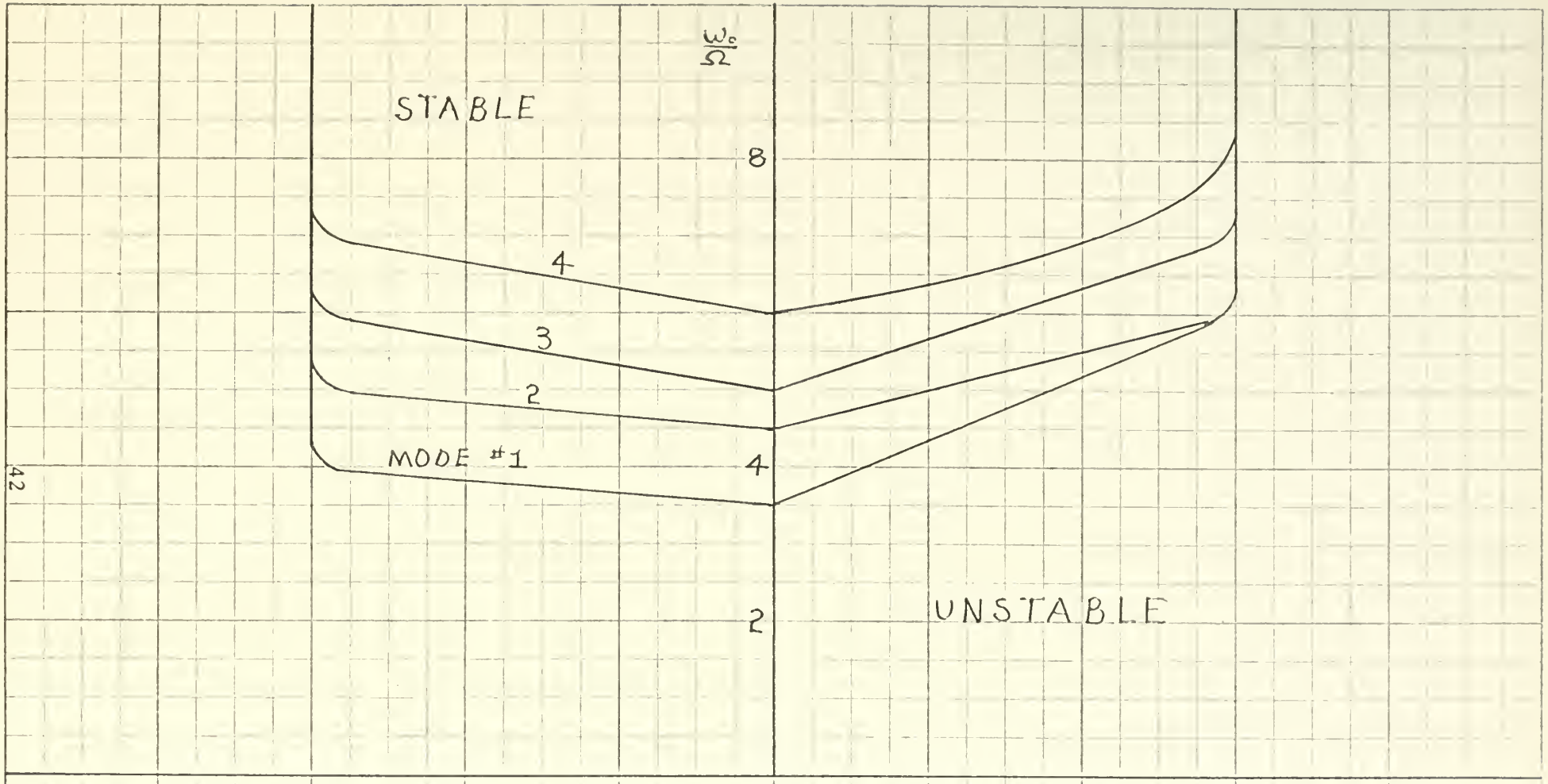

FIGURE 6. STABILITY BOUNDARIES

A.C. 3% CHORD AFT E.A.

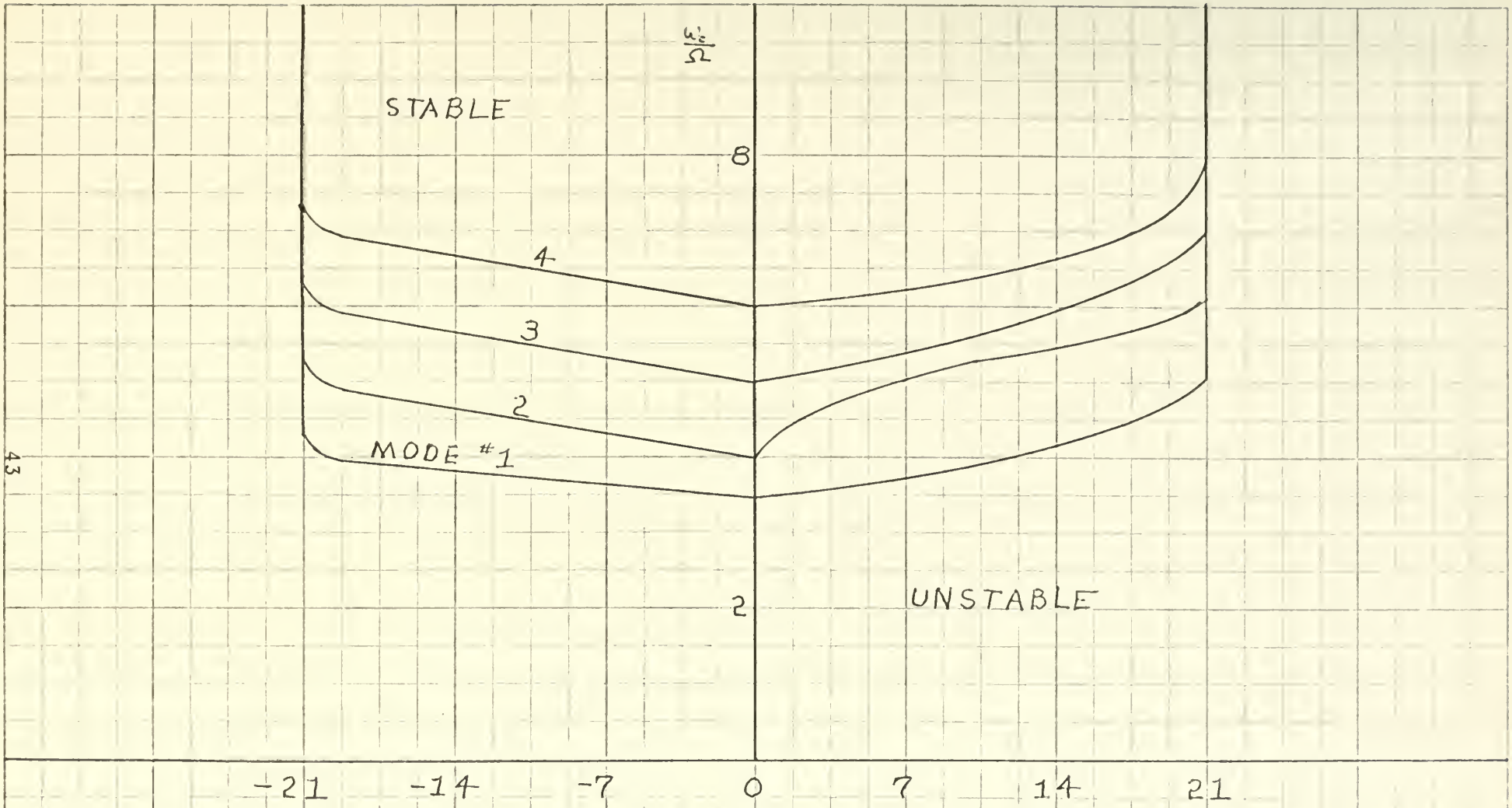

FIGURE 7. STABILITY BOUNDARIES

A.C. 7% CHORD AFT E.A.

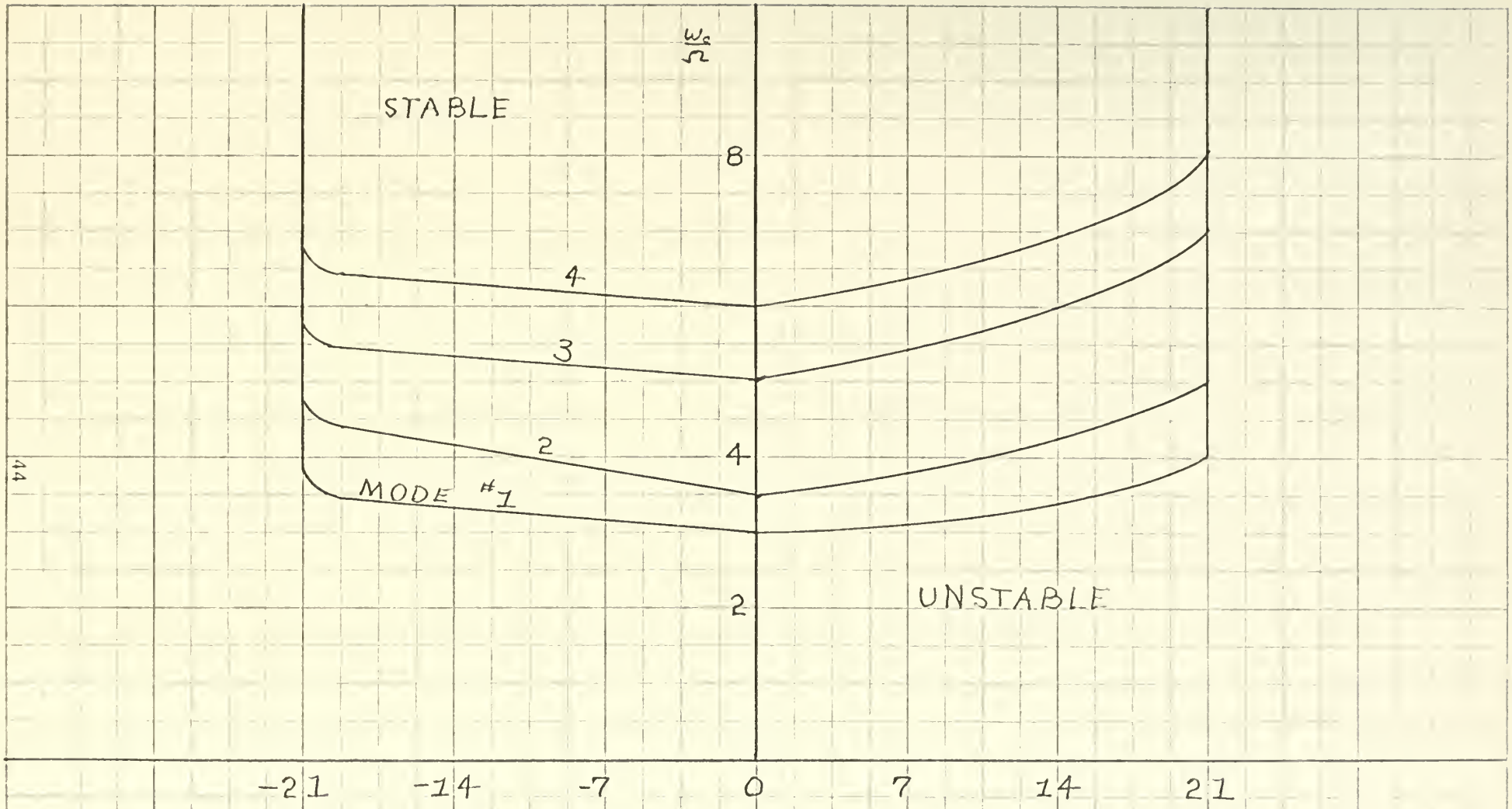

FIGURE 8. STABILITY BOUNDARIES

A.C. 10% CHORD AFT E.A.

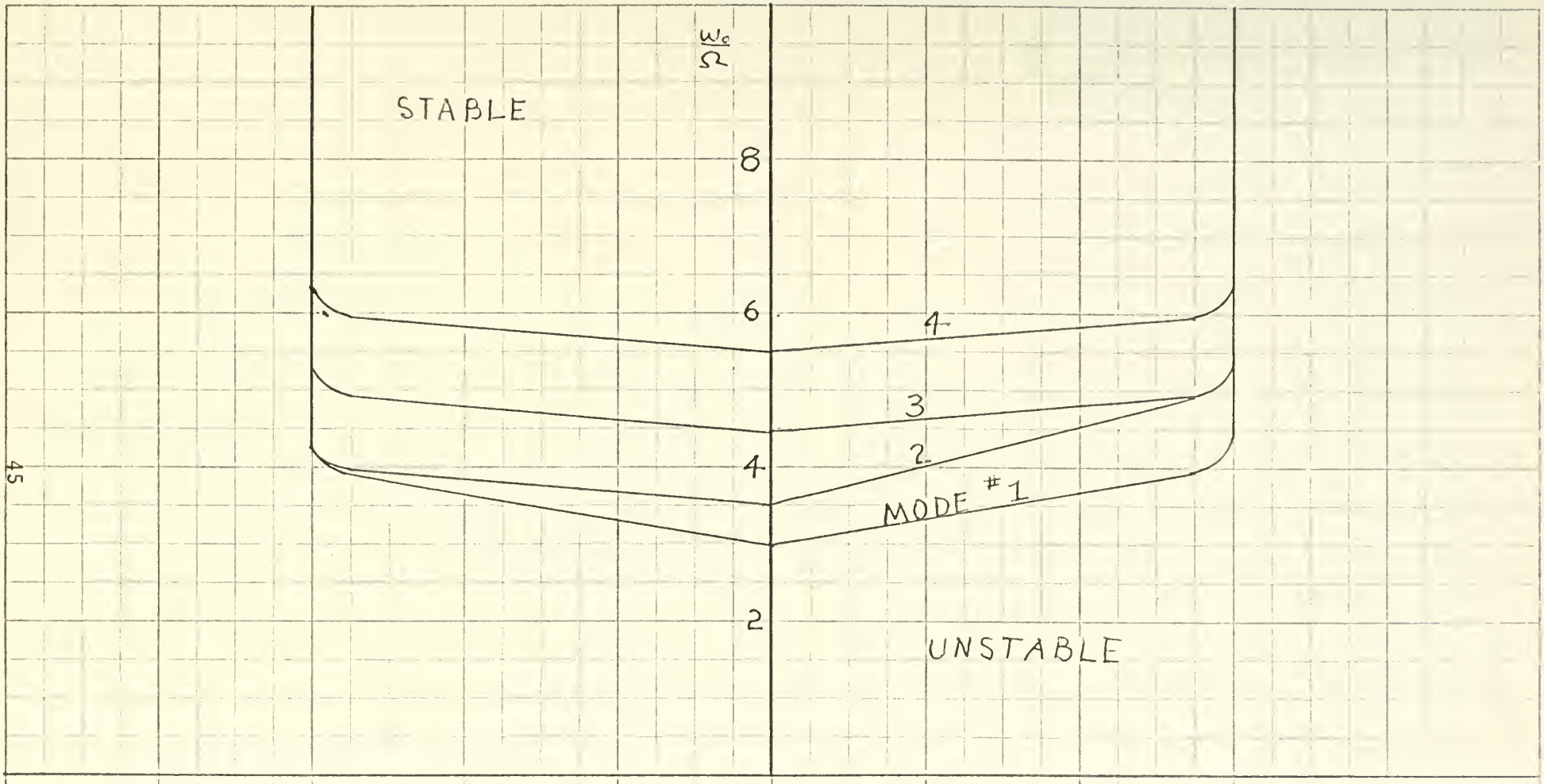

FIGURE 9. STABILITY BOUNDARIES

A.C. 14 % CHORD AFT E.A.

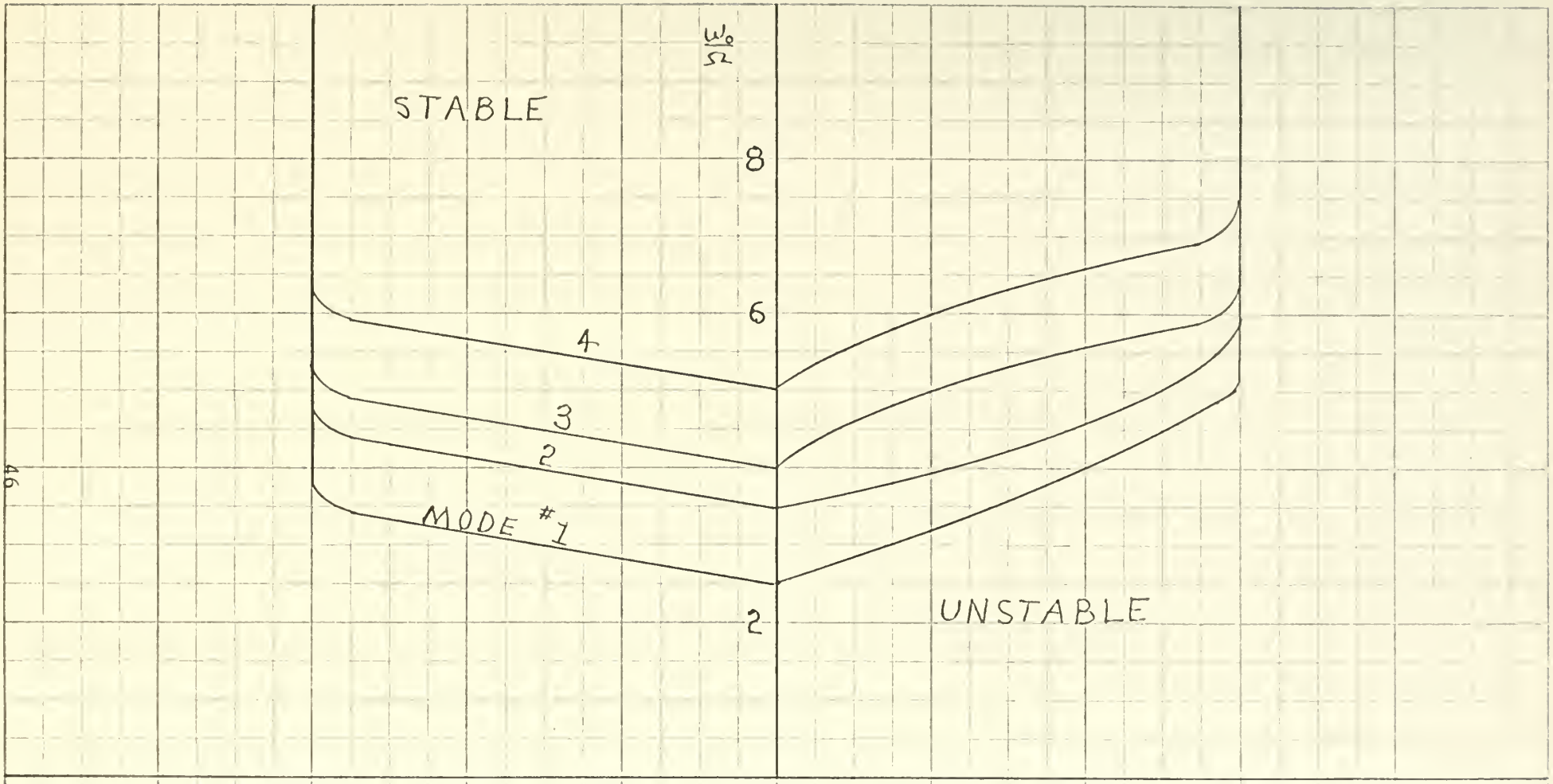

FIGURE 10. STABILITY BOUNDARIES

/ A.C. 17% CHORD AFT E.A.

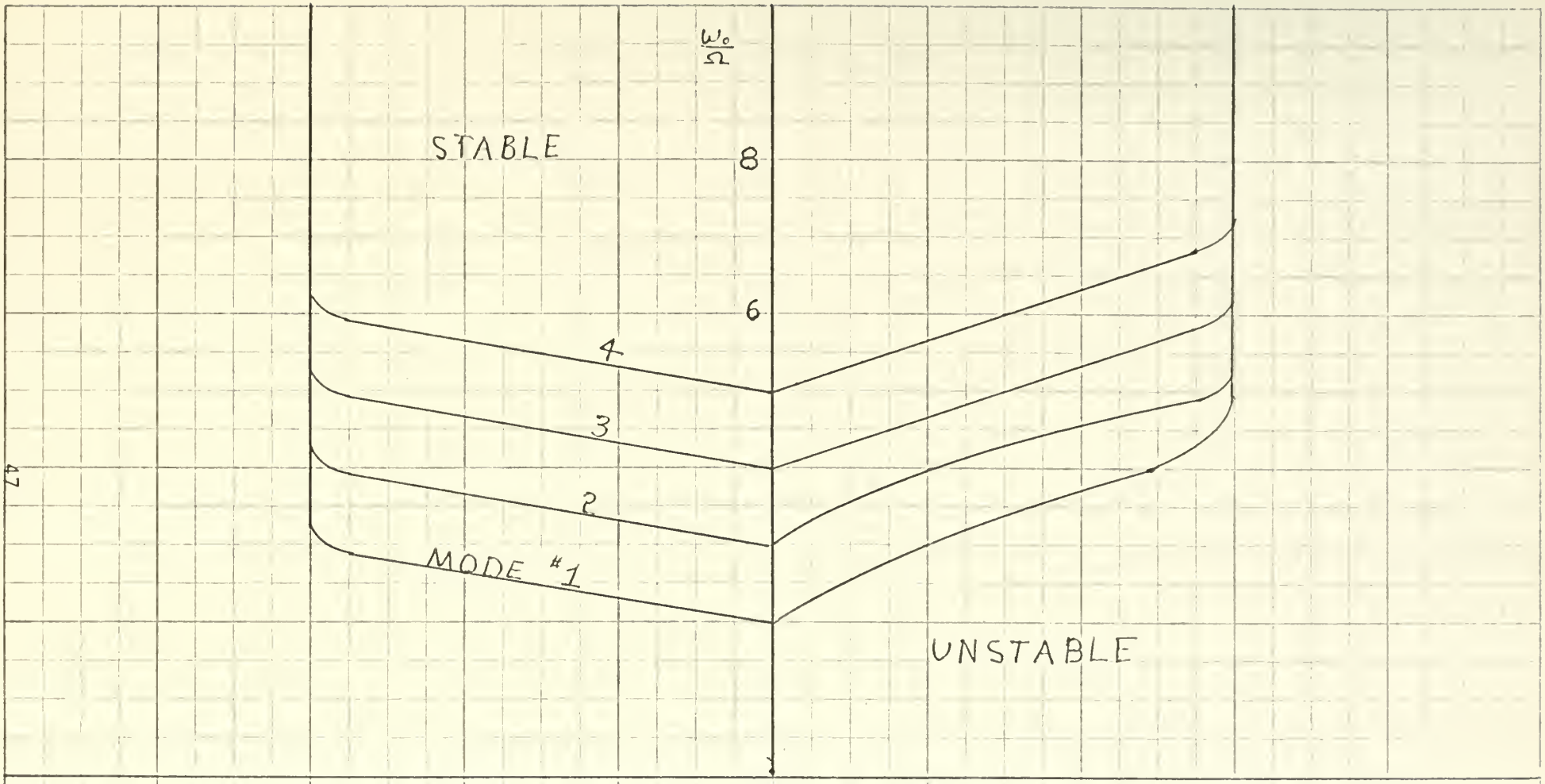

FIGURE 11. STABILITY BOUNDARIES

A.C. 21% CHORD AFT E.A.

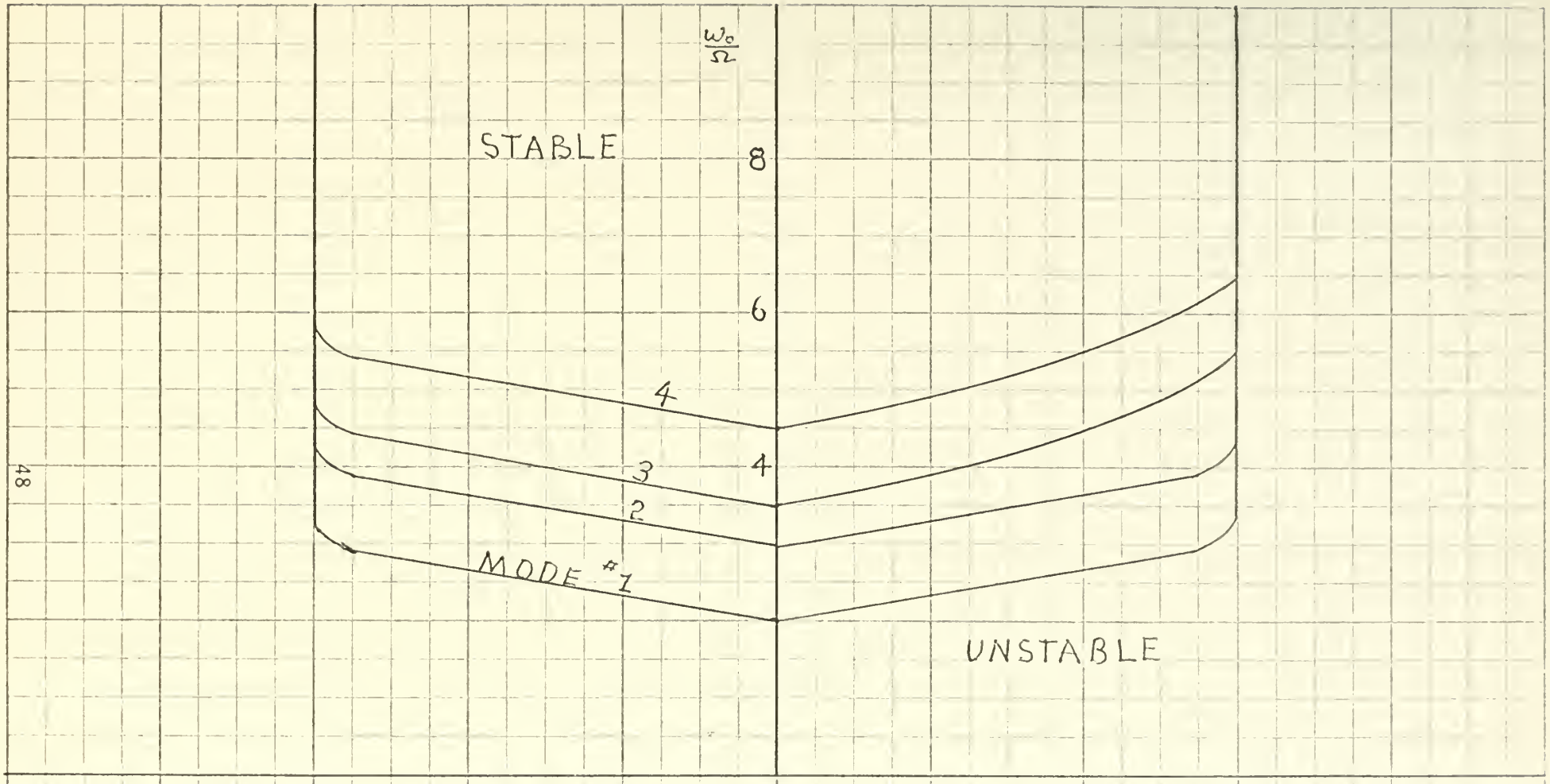

FIGURE 12. STABILITY BOUNDARIES

A.C. 24 % CHORD AFT E.A.

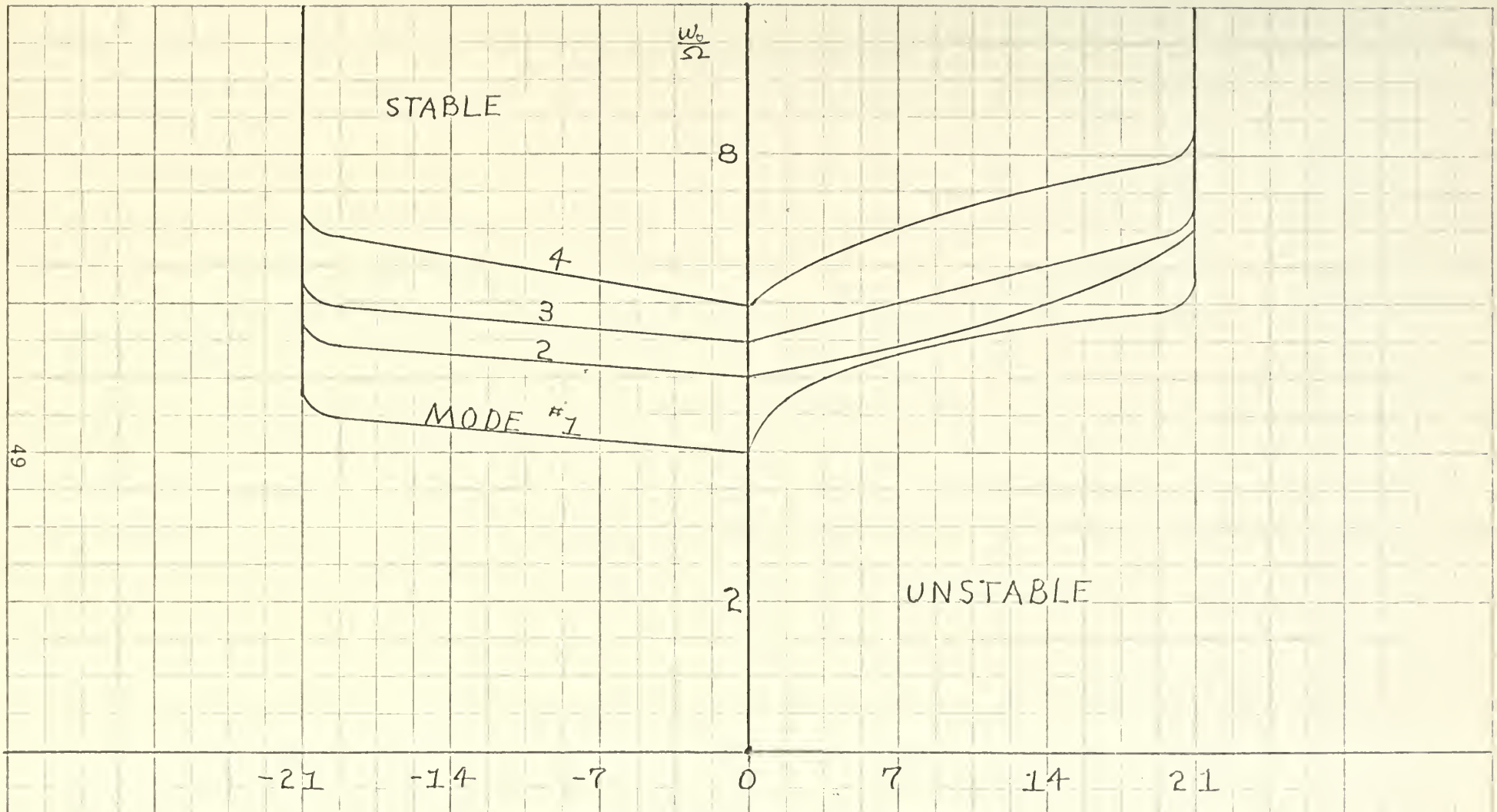

FIGURE 13. STABILITY BOUNDARIES

A.C. 3% CHORD FWD. E.A.

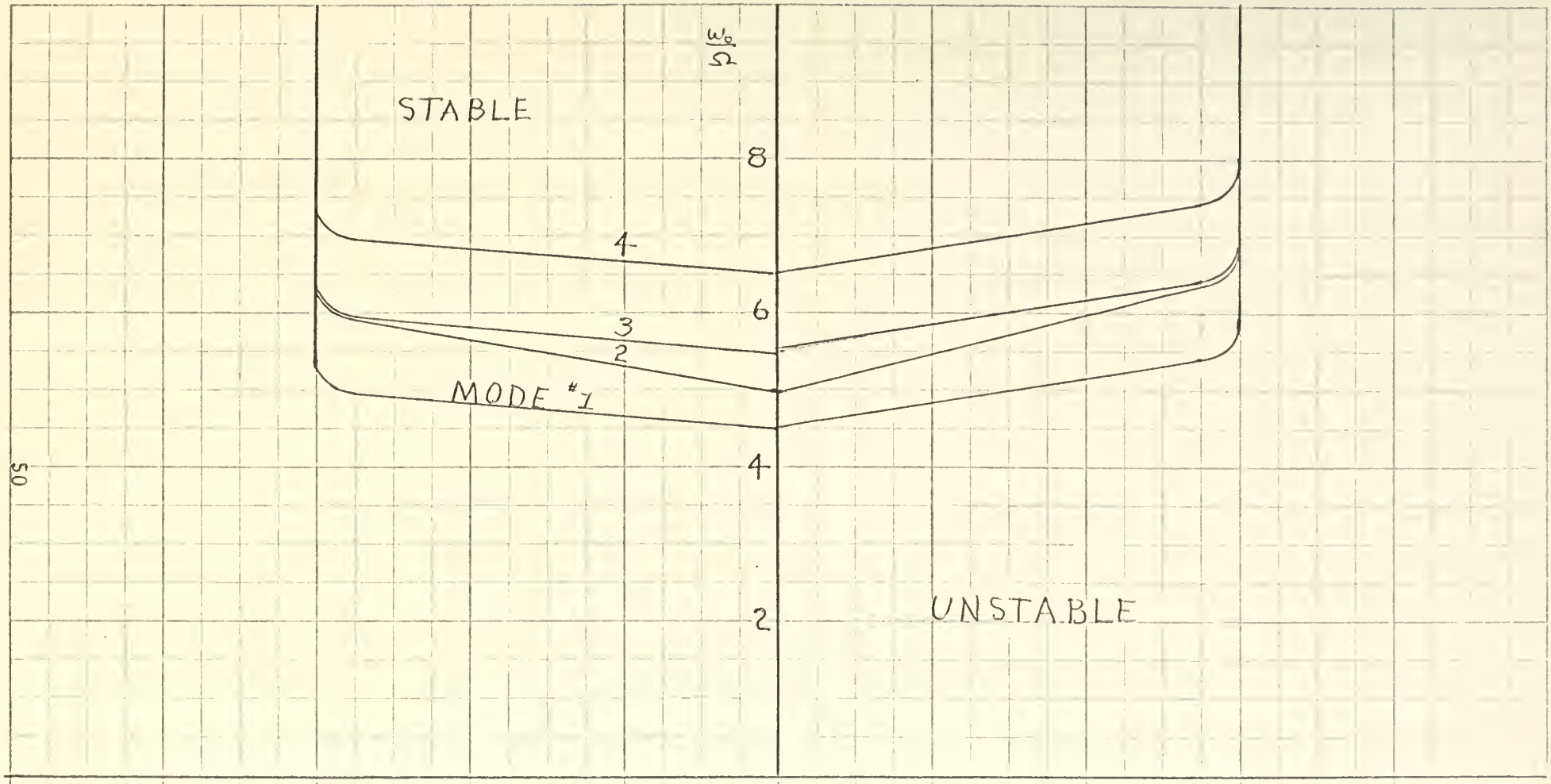

FIGURE 14. STABILITY BOUNDARIES

A.C. 7% CHORD FWD. E.A.

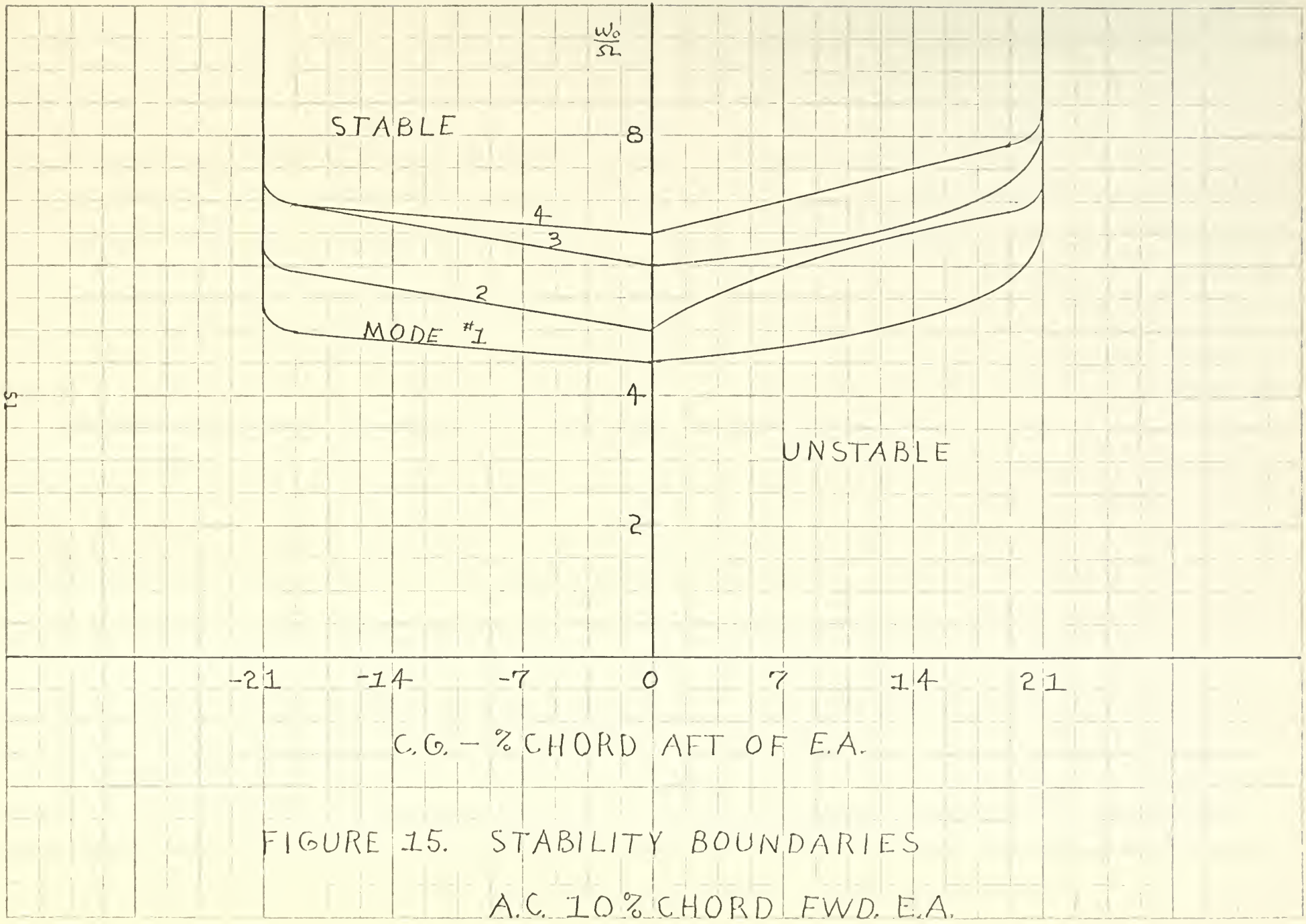

FIGURE 15. STABILITY BOUNDARIES

A.C. 10% CHORD FWD. E.A.

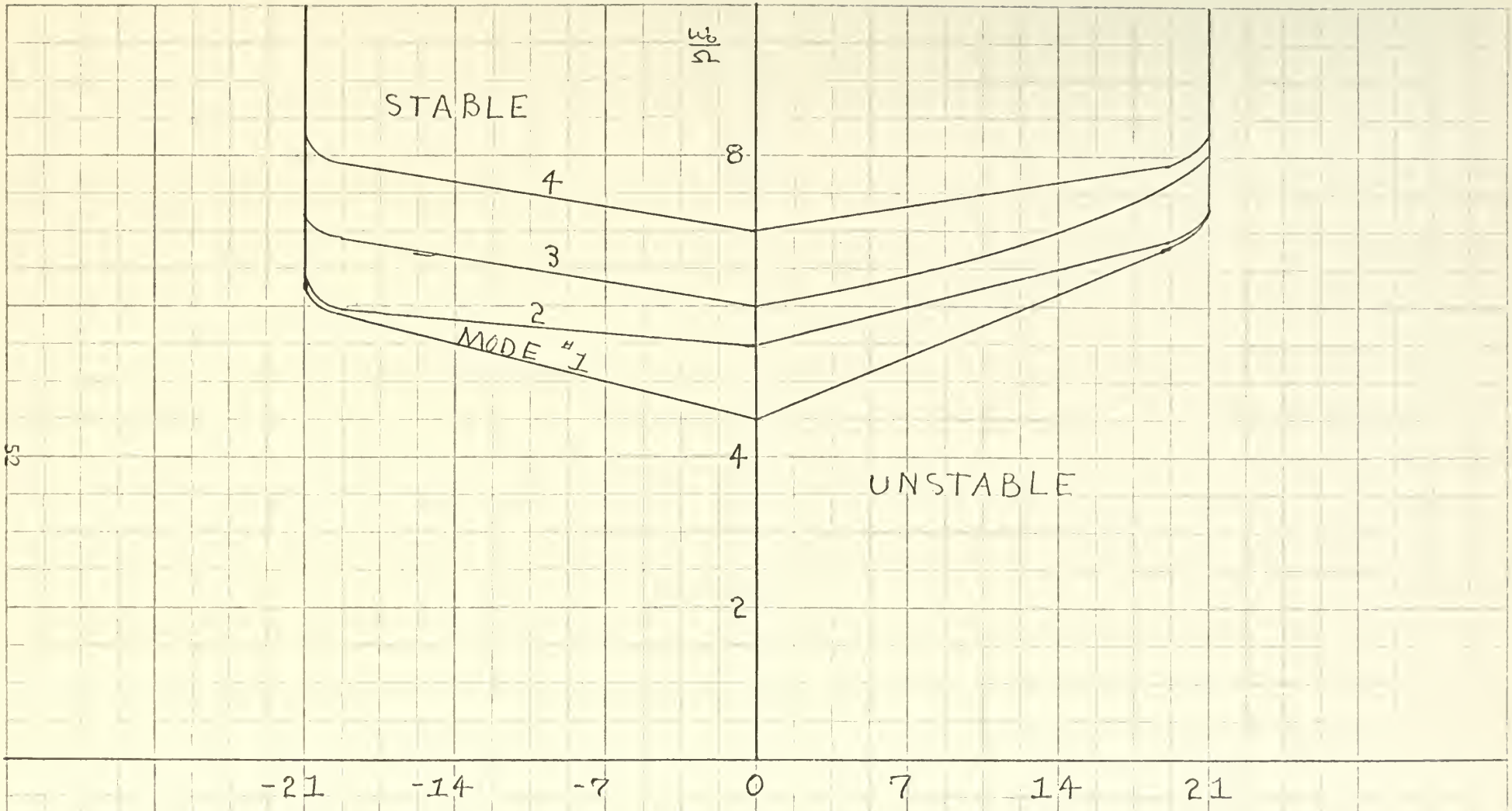

FIGURE 16. STABILITY BOUNDARIES

A.C. 14% CHORD FWD. E.A.

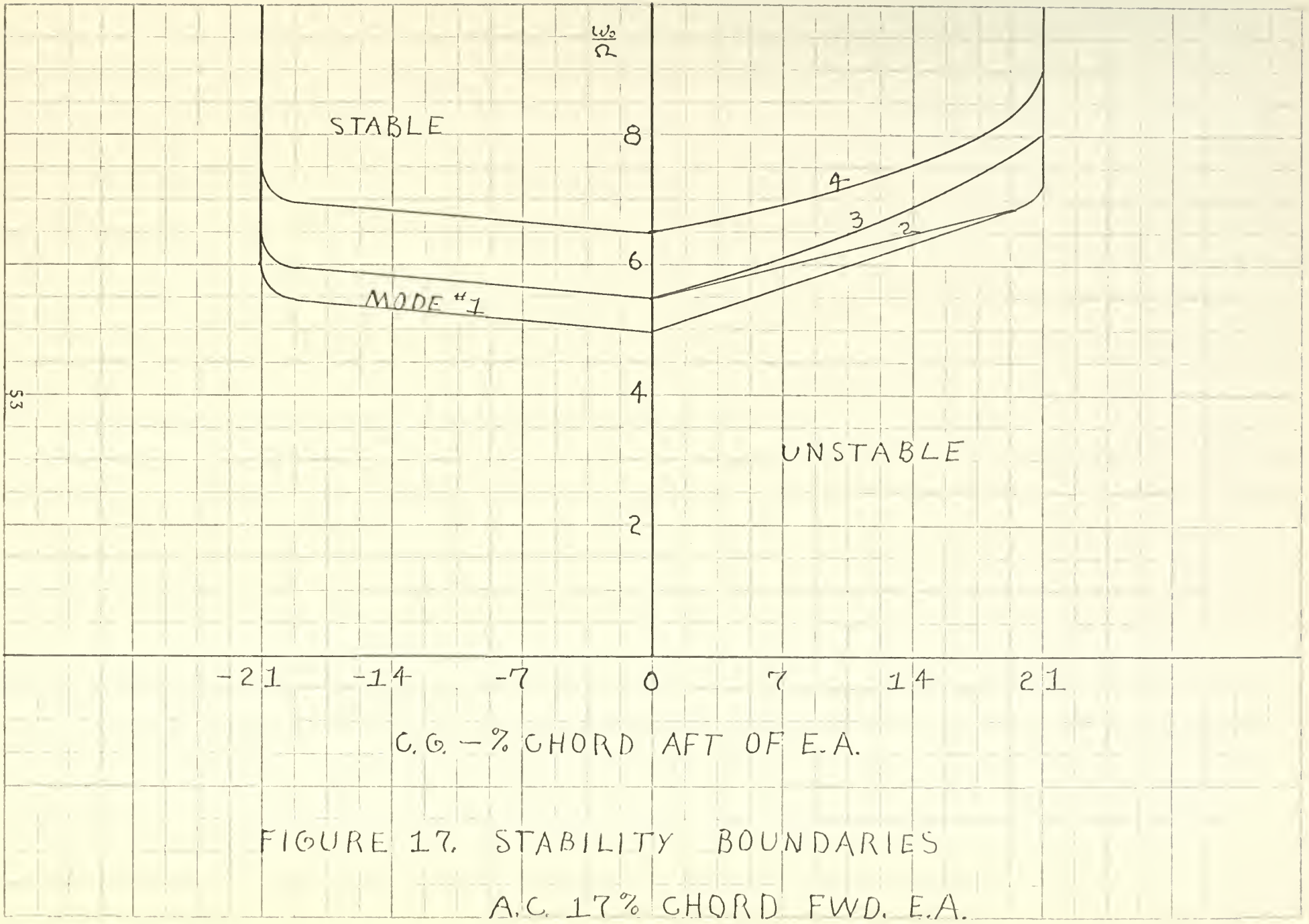

FIGURE 17. STABILITY BOUNDARIES

A.C. 17% CHORD FWD. E.A.

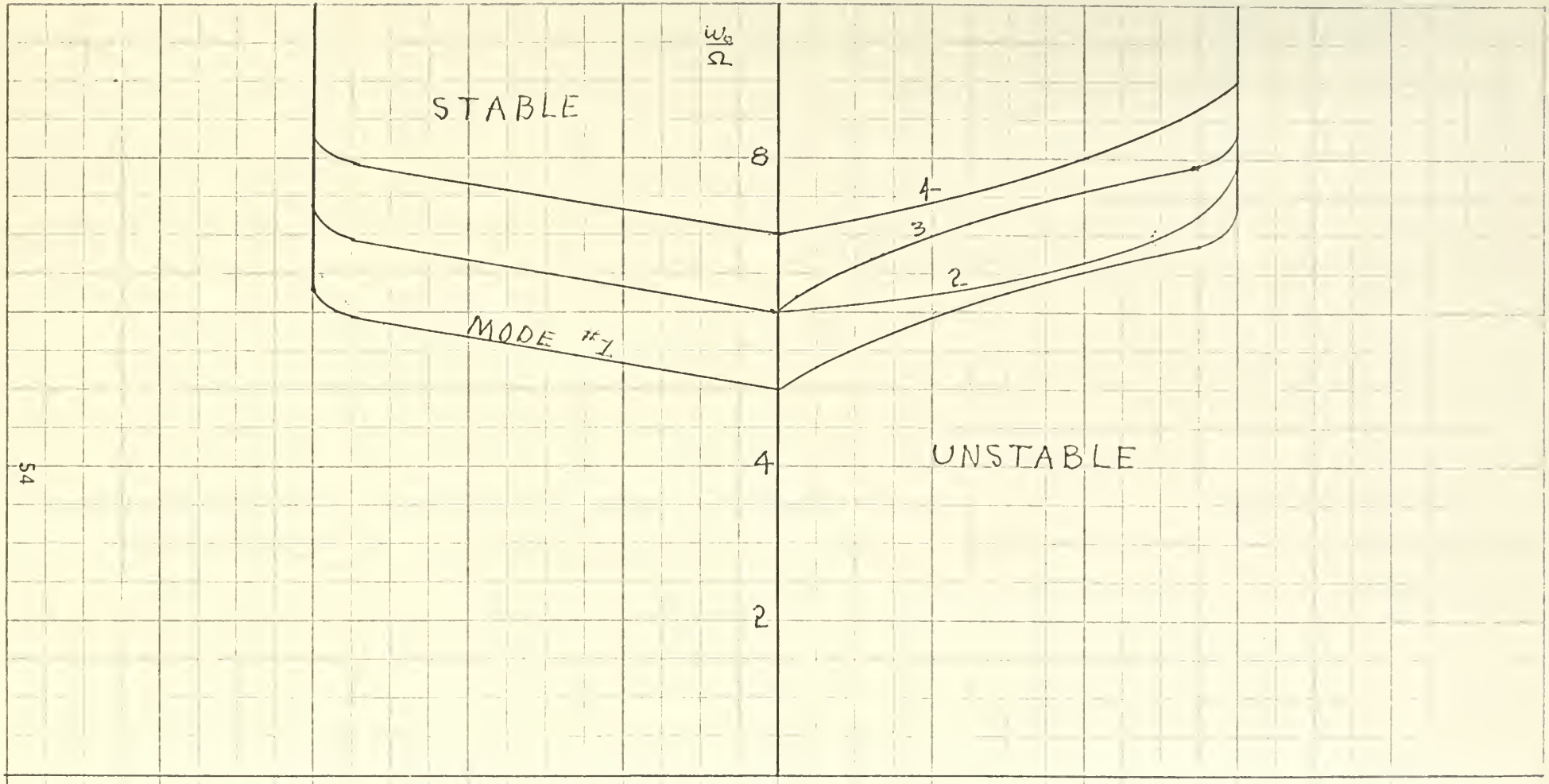

FIGURE 18. STABILITY BOUNDARIES

A.C. 21% CHORD FWD. E.A.

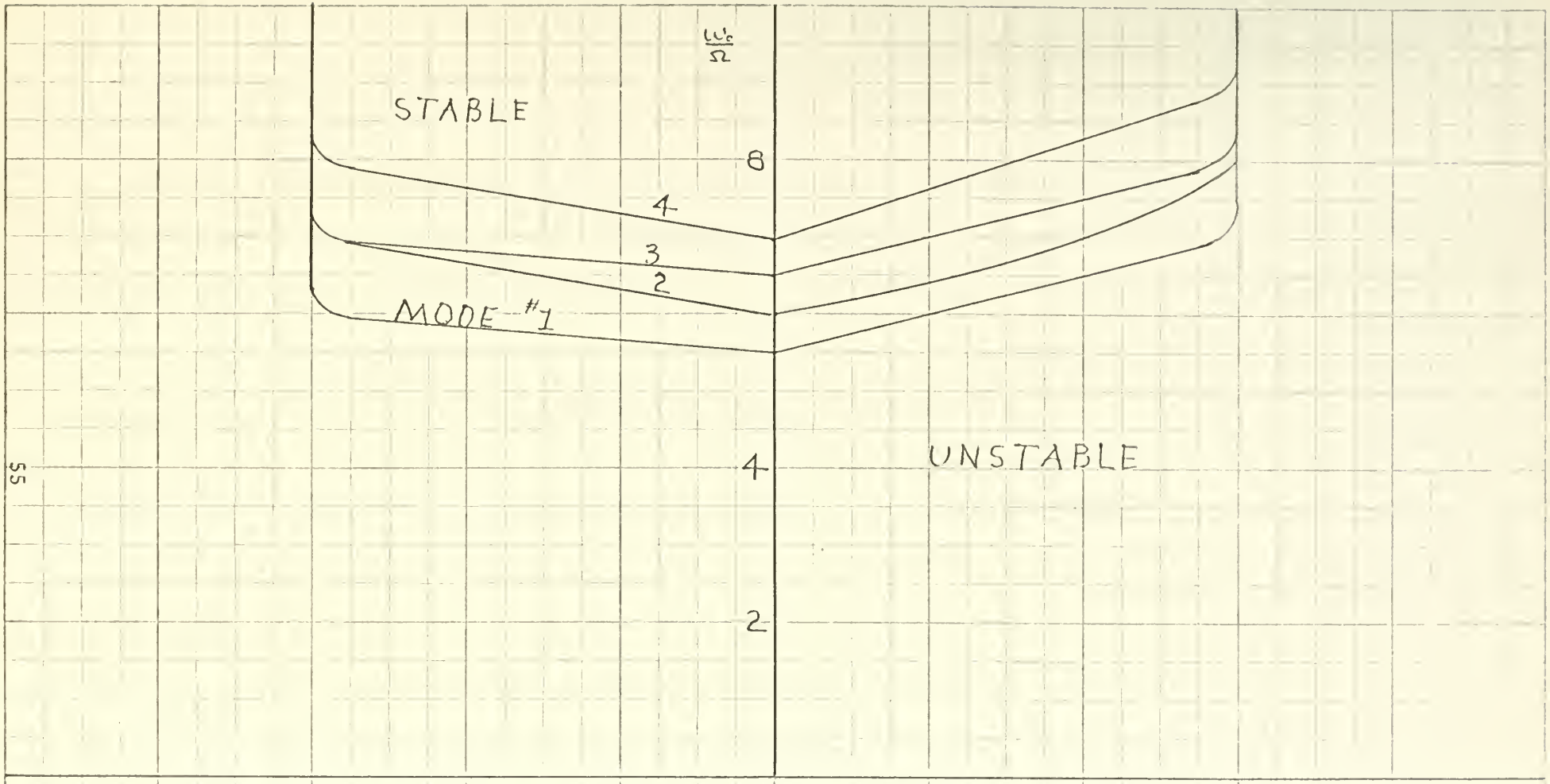

FIGURE 19. STABILITY BOUNDARIES

A.C. 24% CHORD FWD. E.A.

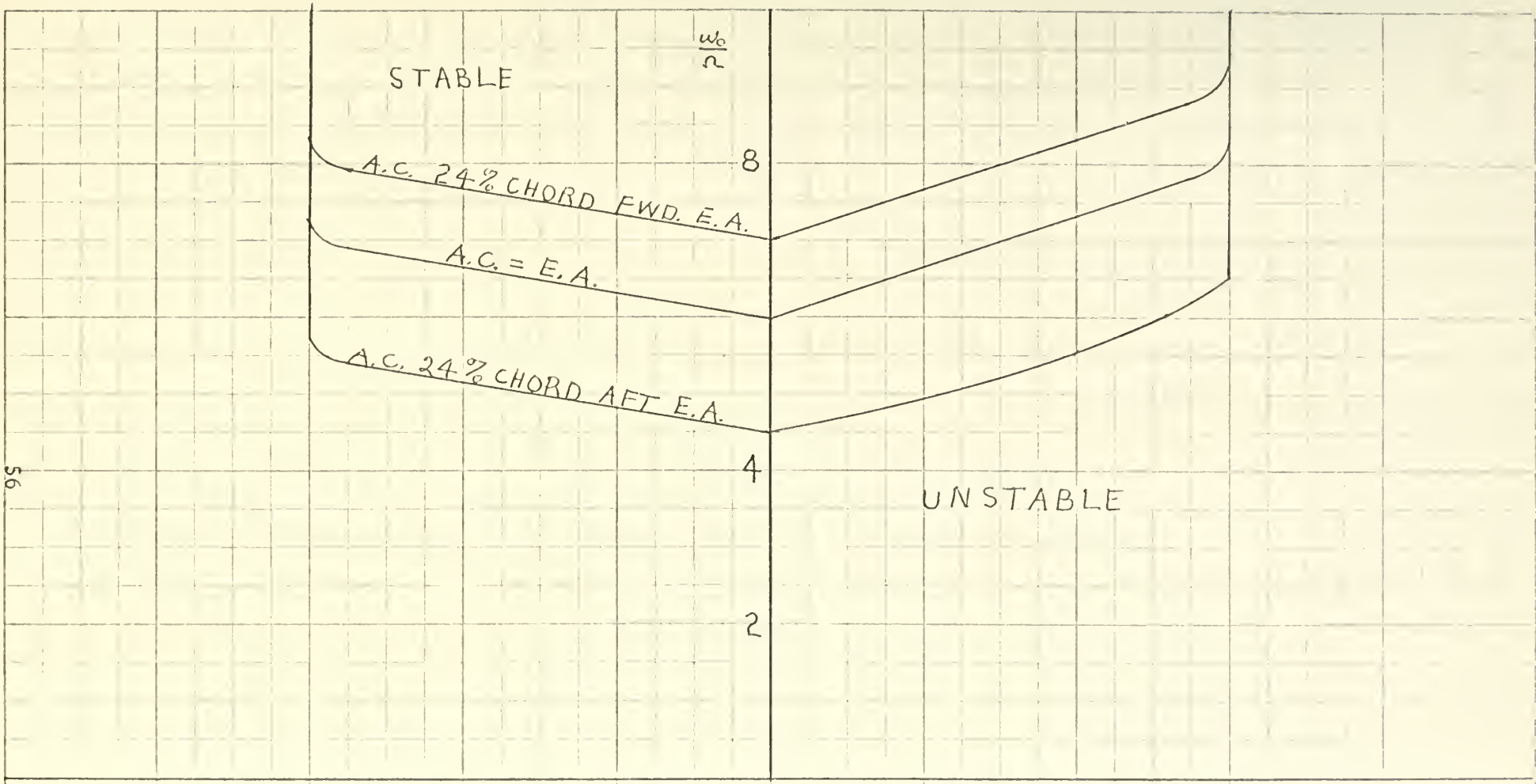

FIGURE 20. STABILITY BOUNDARIES VARYING A.C.

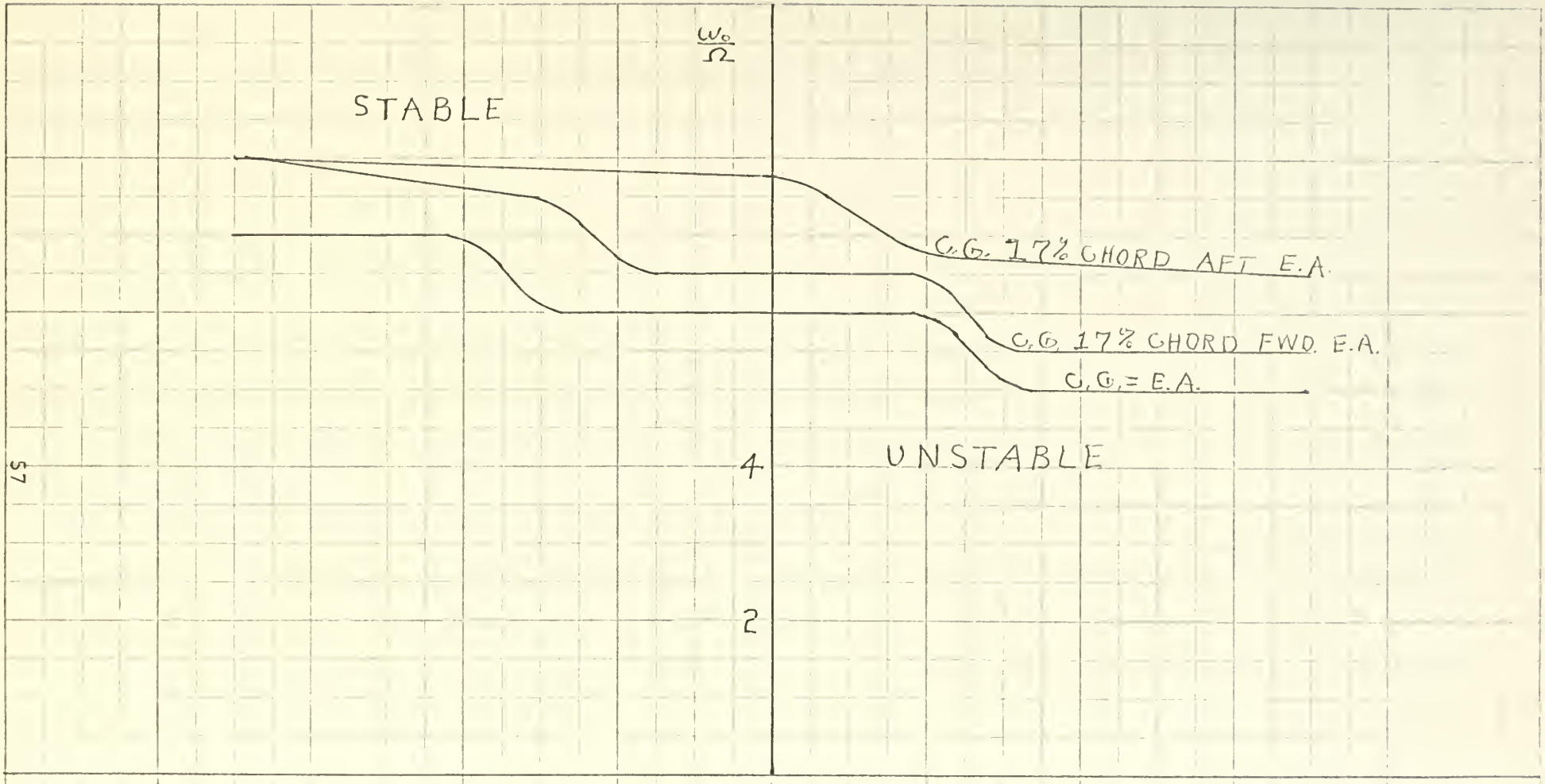

FIGURE 21. STABILITY BOUNDARIES VARYING C.G.

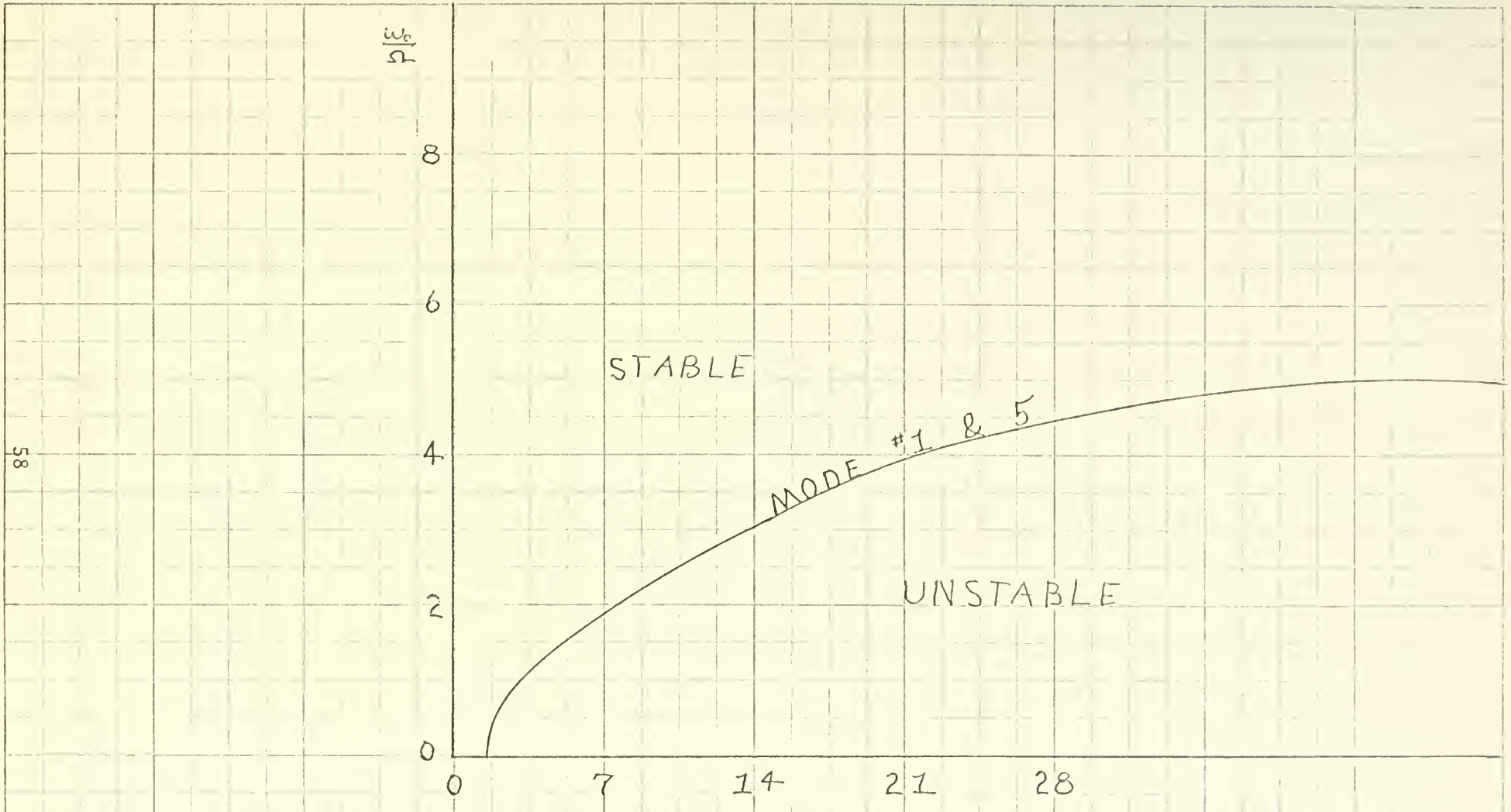

FIGURE 22. DIVERGENCE BOUNDARY

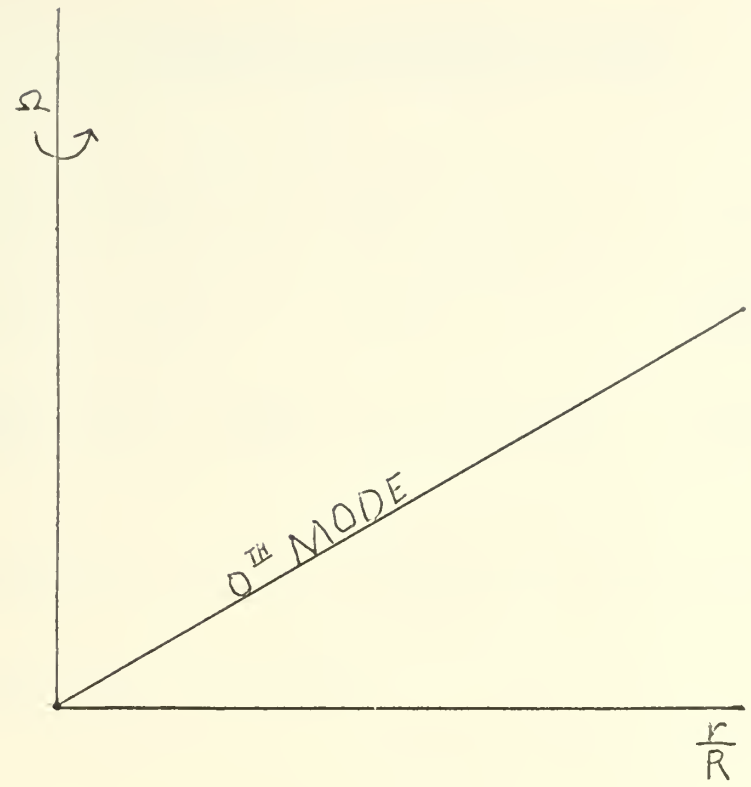

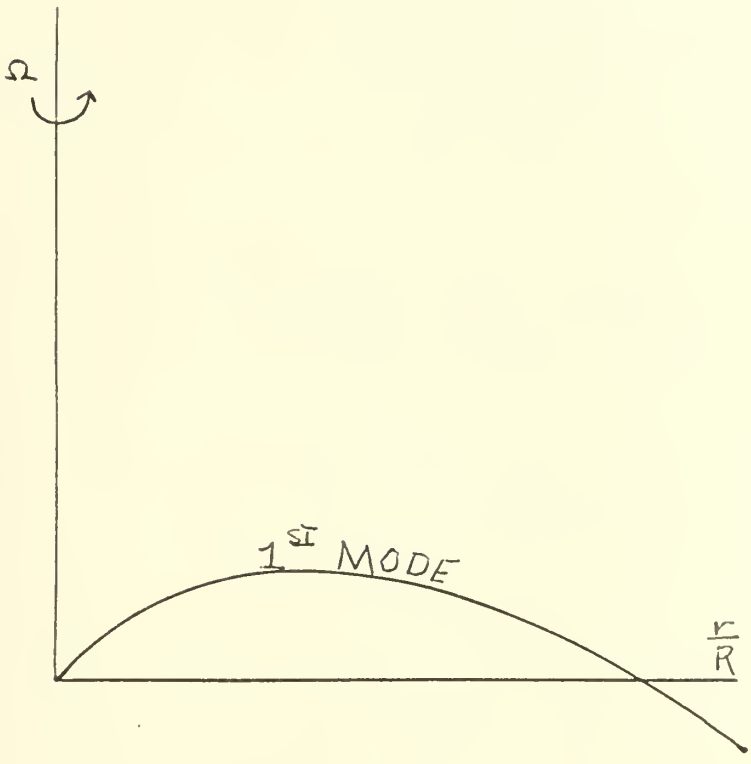

FIGURE 23. FLAPPING MODES

$$\begin{vmatrix} -I_x\nu^2 + m_\theta - I_x & \nu^2 + m_{\dot\beta}\nu + 1 & m_2\nu \\ -I_{x2}\nu^2 + m_{\theta 2} - I_{x2} & m_2\nu & I_2\nu^2 + m_{\dot g}\nu + I_2\nu_2^2 \\ I\nu^2 + M_{\dot\theta}\nu + M_\theta + I + I\left(\frac{\omega_e}{\Omega}\right)^2 & -I_x\nu^2 + M_{\dot\beta}\nu - I_x & -I_{x_2}\nu^2 + M_{\dot g}\nu - I_{x2} \end{vmatrix} = 0$$

EXPANDED, THE CHARACTERISTIC EQUATION IS OF THE FORM:

$$A\nu^6 + B\nu^5 + C\nu^4 + D\nu^3 + E\nu^2 + F\nu + G$$

WHERE,

$$A = II_2 - I_{x2}^2 - I_x^2 I_2$$

$$B = 2I_x I_{x2} m_2 + I_x I_2 M_{\dot\beta} - I_x^2 m_{\dot g} + I_x M_{\dot g} + I_2 M_{\dot\theta} - I_{x2}^2 m_{\dot\beta} + II_2 m_{\dot\beta}$$

$$C = -I_x m_2 M_{\dot g} + I_x m_{\dot g} M_{\dot\beta} - I_x^2 I_2 \nu_2^2 + I_x I_2 m_\theta - 2I_{x2}^2 + I_{x2} m_{\theta 2} + I_{x2} I_2 + I_2 M_\theta + 2II_2 + II_2\left(\frac{\omega_e}{\Omega}\right)^2 + M_{\dot\theta} m_{\dot g} + II_2\nu_2^2 + I_x M_{\dot g} m_{\dot\beta} + I_2 M_{\dot\theta} m_{\dot\beta} + I m_{\dot g} m_{\dot\beta} - I_{x2} M_{\dot\beta} m_2 - I m_2^2$$

$$D = 4I_x I_{x2} m_2 - 2I_x^2 m_{\dot g} + I_x I_2 M_{\dot\beta}\nu_2^2 - I_{x2} m_2 m_\theta - I_2 M_{\dot\beta} m_\theta + I_x m_{\dot g} m_\theta + I_x I_2 M_{\dot\beta} - m_{\theta 2} M_{\dot g} + I_{x2} M_{\dot g} + M_\theta m_{\dot g} + 2I m_{\dot g} + I\left(\frac{\omega_e}{\Omega}\right)^2 m_{\dot g} + I_2 M_{\dot\theta}\nu_2^2 - I_{x2}^2 m_{\dot\beta} + I_x m_{\theta 2} m_{\dot\beta} + I_{x2} I_2 m_{\dot\beta} + I_2 M_\theta m_{\dot\beta} - II_2 m_{\dot\beta} + II_2\left(\frac{\omega_e}{\Omega}\right)^2 m_{\dot\beta} + M_{\dot\theta} m_{\dot g} m_{\dot\beta} + II_2\nu_2^2 m_{\dot\beta}$$

$$+I_x M_{\dot{g}} + I_2 M_{\dot{\theta}} - I_x m_{o2} m_2 - M_{\dot{\theta}} m_2^2$$

$$E = -2I_x^2 I_2 v_2^2 + m_\theta m_2 M_{\dot{g}} + I_x I_2 m_\theta - m_\theta m_{\dot{g}} M_{\dot{\beta}} + I_x I_2 m_\theta v_2^2 - I_x m_2 M_{\dot{g}} - I_x^2 I_2 + I_x m_{\dot{g}} M_{\dot{\beta}} + I_2 m_{\theta 2} + I_2 M_\theta v_2^2 + 2I I_2 v_2^2 + I I_2 \left(\frac{\omega_s}{\Omega}\right)^2 v_2^2 - m_{\theta 2} m_{\dot{\beta}} M_{\dot{g}} + I_{x2} M_{\dot{g}} m_{\dot{\beta}} + M_\theta m_{\dot{g}} m_{\dot{\beta}} + I m_{\dot{g}} m_{\dot{\beta}} + I \left(\frac{\omega_e}{\Omega}\right)^2 m_{\dot{g}} m_{\dot{\beta}} + I_2 M_{\dot{\theta}} m_{\dot{\beta}} v_2^2 - I_{x2}^2 + I_{x2} m_{\theta 2} + I_2 M_\theta + I I_2 + I I_2 \left(\frac{\omega_s}{\Omega}\right)^2 + M_{\dot{\theta}} m_{\dot{g}} + M_{\dot{\beta}} m_{\theta 2} m_2 - I_{x2} M_{\dot{\beta}} m_2 - M_\theta m_2^2 - I m_2^2 - I \left(\frac{\omega_s}{\Omega}\right)^2 m_2$$

$$F = -I_{x2} m_\theta m_2 + I_x m_\theta m_{\dot{g}} - I_2 m_\theta M_{\dot{\beta}} v_2^2 + 2 I_x I_{x2} m_2 - I_x^2 m_{\dot{g}} + I_x I_2 M_{\dot{\beta}} v_2^2 + I_2 m_{\theta 2} m_{\dot{\beta}} - I_{x2} I_2 m_{\dot{\beta}} + I_2 M_\theta m_{\dot{\beta}} v_2^2 + I I_2 m_{\dot{\beta}} v_2^2 + I I_2 \left(\frac{\omega_e}{\Omega}\right)^2 m_{\dot{\beta}} v_2^2 - m_{\theta 2} M_{\dot{g}} + I_{x2} M_{\dot{g}} + M_\theta m_{\dot{g}} + I m_{\dot{g}} + I \left(\frac{\omega_e}{\Omega}\right)^2 m_{\dot{g}} + I_2 M_{\dot{\theta}} v_2^2 - I_x m_{\theta 2} m_2$$

$$G = I_x I_2 m_\theta v_2^2 - I_x^2 I_2 v_2^2 + I_2 m_{\theta 2} - I_{x2} I_2 + I_2 M_\theta v_2^2 + I I_2 v_2^2 + I I_2 \left(\frac{\omega_e}{\Omega}\right)^2 v_2^2$$

APPENDIX II--ROUTH'S ARRAY

To establish stability of the rotating helicopter blade, with three modes of motion, Routh's criteria was used. In order to use Routh's Criteria, Routh's array had to be set up. The form of the characteristic equation was:

$$A\nu^6 + B\nu^5 + C\nu^4 + D\nu^3 + E\nu^2 + F\nu + G = 0 \qquad \text{(III)}$$

This leads to an array of the following form:

ν^6	A	C	E	G
ν^5	B	D	F	
ν^4	A_1	B_1	G	
ν^3	A_2	B_2		
ν^2	A_3	G		
ν^1	A_4			
ν^0	G			

where

$$A_1 = \frac{BC - AD}{B}$$

$$B_1 = \frac{BE - AF}{B}$$

$$A_2 = \frac{A_1D - BB_1}{A_1}$$

$$B_2 = \frac{A_1F - BG}{A_1}$$

$$A_3 = \frac{A_2B_1 - A_1B_2}{A_2}$$

and

$$A_4 = \frac{A_3 B_2 - A_2 G}{A_3}$$

APPENDIX III--ROTOR BLADE DATA

Cornell Aero Lab Blade #1

NACA 0012 Airfoil

Radius = 48 inches

Chord = 3.5 inches

Weight = 2.5 pounds

$I = .000479$ slug feet ^{2}

$I_b = 1.66$ slug feet ^{3}

$\nu = 2.46$

APPENDIX IV--TERMS OF EQUATIONS OF MOTION

I. Flapping and Flap-Bending Equations

1. β and g terms.

These terms arise from the z - component of the centrifugal force at each blade element. A virtual deflection of $\delta\beta$ or δg results in energy being expended which results in a force for the whole blade of

$$\Omega^2 I_b \beta \tag{IV1}$$

$$M_2 \Omega^2 \nu_2^2 g \tag{IV2}$$

2. θ term.

Due to a twist of the blade, the centrifugal force of a blade element, $Mr\Omega^2 dr$, will act with a moment arm, $-\eta_k X_I dr\theta$, resulting in a force of

$$-\int_0^R m\Omega^2 \eta_k X_I \, dr\, \theta \tag{IV3}$$

3. $\ddot{\beta}$ and $\ddot{g}$ term.

At each blade element there is an intertial force of

$$mr\ddot{\beta}dr$$
$$mr\ddot{g}dr$$

which results in a force of

$$I_b \ddot{\beta} \tag{IV4}$$

$$M_2 \ddot{g} \tag{IV5}$$

4. $\ddot{\theta}$ term.

Due to a pitching acceleration there is an inertial effect which results in the following force.

$$-\int_0^R m\Omega^2 \eta_k X_I \, dr\, \ddot{\theta} \tag{IV6}$$

5. θ term, aerodynamic.

This term is due to a twist angle, θ, which causes energy to be transmitted by the airstream to the blade giving a force of

$$I_b \Omega^2 m_\theta \theta \tag{IV7}$$

and

$$I_b \Omega^2 m_{\theta 2} \theta \tag{IV8}$$

6. $\dot{\beta}$ and $\dot{g}$ terms.

The flapping velocity at each blade element causes a relative change in the angle of attack which results in the following forces:

$$\Omega m_{\dot{\beta}} \dot{\beta} \tag{IV9}$$

$$\Omega m_{\dot{g}} \dot{g} \tag{IV10}$$

$$\Omega m_2 \dot{g} \tag{IV11}$$

$$\Omega m_2 \dot{\beta} \tag{IV12}$$

II. Pitching Equation

1. β term.

Due to a virtual twist of the blade, the z - component of the centrifugal force of a blade element causes a force of

$$-\int_o^R m \Omega^2 \eta_k x_I \, dr \, \beta \tag{IV13}$$

2. θ terms.

This term arises from the "tennis racket" effect. Each partical of mass, dm, of a blade section is acted upon - due to a twist deflection - by a component of the centrifugal force in the plane of the section. The resulting force is

$$\left[I_\theta \Omega^2 + I_\theta \omega_o^2 \right] \theta \tag{IV14}$$

3. $\ddot{\beta}$ term.

Due to a virtual deflection of a blade section, the inertia force, $mr\ddot{\beta}dr$, results in a force of

$$-\int_0^R m\Omega^2 \eta_k \chi_I \, dr \, \ddot{\beta} \tag{IV15}$$

4. $\ddot{\theta}$ term.

This force arises from the inertia force due to a twist of the blade.

$$I_\theta \Omega^2 \ddot{\theta} \tag{IV16}$$

5. $\dot{\beta}$ term.

This aerodynamic term is the result of a couple produced by the pitching acceleration of the rotor blade.

$$M_{\dot{\beta}} I_b \Omega \dot{\beta} \tag{IV17}$$

6. $\dot{\theta}$ term.

This aerodynamic term is the result of the energy transmitted to the blade by the lift forces moving through a virtual displacement.

$$M_{\dot{\theta}} I_b \Omega \dot{\theta} \tag{IV18}$$

Thesis 129281
S877 Swah
A theoretical analysis of the effect of the modulus of elasticity and other parameters upon the flutter of a helicopter rotor-blade in hovering flight.